BioMed Research International

Advances in Biotechnology for Sustainable Development

Guest Editors: Weiqi Fu, Basel Khraiwesh, Hongbing Liu, and Lei Kai

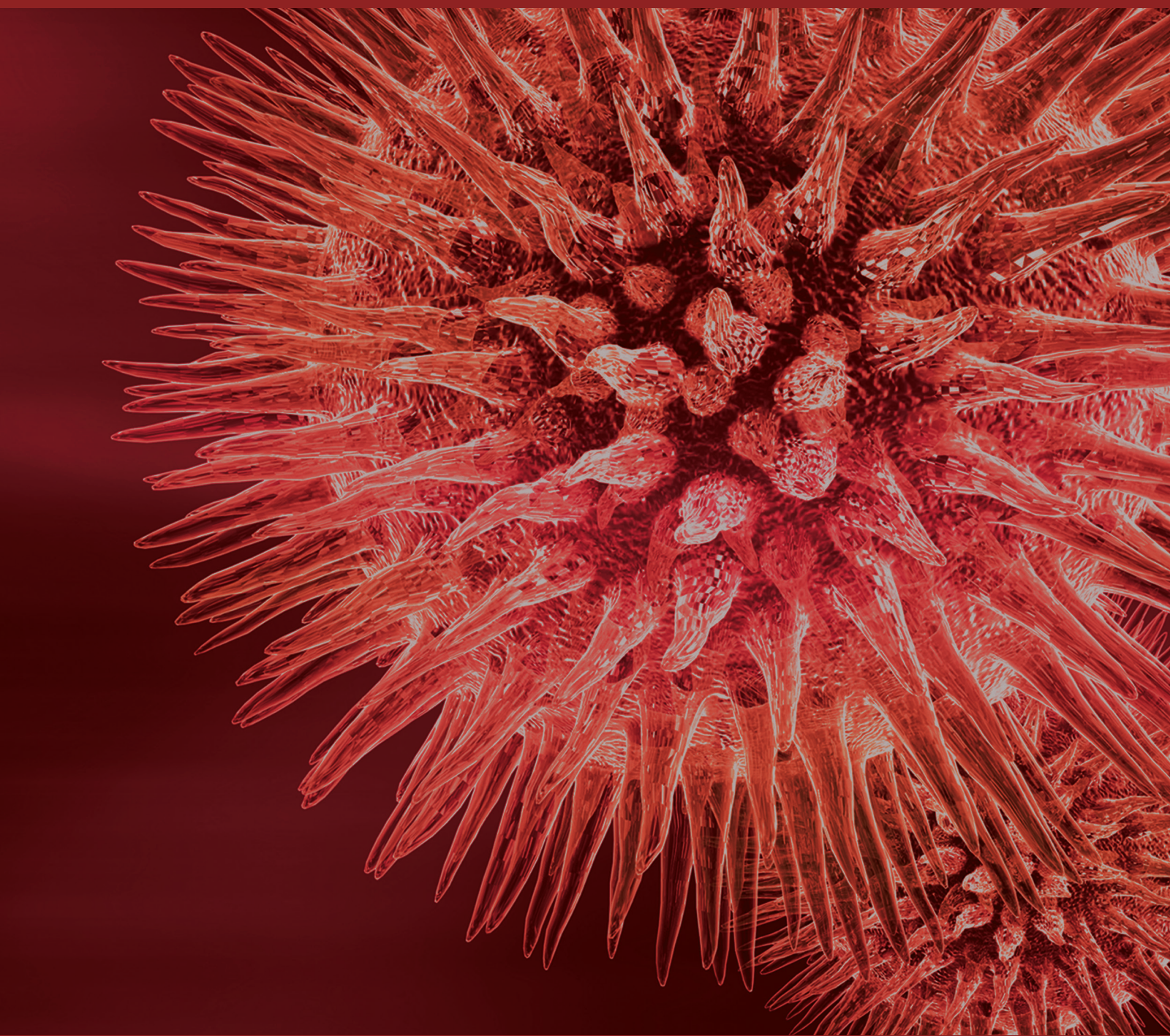

Advances in Biotechnology for Sustainable Development

BioMed Research International

Advances in Biotechnology for Sustainable Development

Guest Editors: Weiqi Fu, Basel Khraiwesh, Hongbing Liu, and Lei Kai

Contents

Hindawi Publishing Corporation
BioMed Research International
Volume 2016, Article ID 7154916, 2 pages
http://dx.doi.org/10.1155/2016/7154916

Editorial

Advances in Biotechnology for Sustainable Development

Weiqi Fu,[1,2] Basel Khraiwesh,[1] Hongbing Liu,[3] and Lei Kai[4]

[1]*Division of Science and Math and Center for Genomics and Systems Biology (CGSB), New York University Abu Dhabi, P.O. Box 129188, Abu Dhabi, UAE*
[2]*Center for Systems Biology and Faculty of Industrial Engineering, Mechanical Engineering and Computer Science, School of Engineering and Natural Sciences, University of Iceland, 101 Reykjavik, Iceland*
[3]*National Institute of Diabetes and Digestive and Kidney Diseases (NIDDK), National Institutes of Health (NIH), 9000 Rockville Pike, MD 20892, USA*
[4]*Max Planck Institute of Biochemistry, 82152 Martinsried, Germany*

Correspondence should be addressed to Weiqi Fu; wf21@nyu.edu

Received 9 March 2016; Accepted 10 March 2016

It may be mentioned that transformation towards a biobased industry is one of the big challenges facing our human society. Biotechnology is such a driver for change from petroleum-based economy to a more sustainable biobased economy. The use and development of biotechnologies for bioproduction and bioremediation are of great interest across a wide range of different communities. Moreover, during the past decades, development of tools in manipulating genetic framework empowered the cell factories as a reliable bioresource of recombinant protein production. The number of organisms that can be used as expression system is expanding. *Escherichia coli* was the most studied and used platform organism, then followed by the implementation of yeast as a eukaryotic model organism. Recently, algal cells, insect cells, and mammalian cells are catching up with their abilities of posttranslational modifications. In addition to the living cells, *in vitro* protein production is also emerging as one important tool for recombinant protein production, especially in membrane proteins, toxins, and aggregation prone proteins. Using cell lysate or purified proteins as the source of transcription and translation machinery, corresponding recombinant proteins of certain genes can be produced within several hours. The boosts of recombinant protein production develop along with the biophysics methods. Nuclear magnetic resonance (NMR) and liquid chromatography-mass spectrometry (LC-MS) are now routinely used as identification and characterization of recombinant proteins. Though the topics and papers selected here are not a fully comprehensive representation of the research area of biotechnology for sustainable development, we believe that the rich knowledge presented in these quality papers should be shared with the scientific community in the related fields.

This special issue received a submission of twenty-three manuscripts with an acceptance rate of approximately 22%. The specific papers are described with details as below.

The paper authored by R. Elkacmi et al. developed a quick and easy separation process for extracting oleic acid with high purity, biodegradable soap with a very good quality as well as glycerol from olive mill wastewater, which could cause detrimental effects on nature. It could recover valuable products with an industrial scale. However, so much waste going into the environment is neither reusable nor recyclable, so phytoremediation remains one of the best choices to clean up our environment.

The paper authored by H. Mubarak et al. presented an interesting work on the metabolic modifications in the species *Boehmeria nivea* L. subjected to different levels of the arsenic (As) concentration under hydroponic conditions. The cellular basis of the As tolerance in *B. nivea* L. is well explained. We should believe that, with emerging technologies designed specifically for protecting the environment, the globe will become clean and clear gradually again.

The paper authored by X. Zheng and D. Li studied the synergistic effects between *Rhizobium phaseoli* and

Acidithiobacillus ferrooxidans in the bioleaching process of copper. The work presented demonstrated that mixed cultures using high-tolerance chemoheterotrophic bacteria achieved better performance than pure cultures in bioleaching process and suggested a method to address the challenge of low leaching rate and inefficiency.

The paper authored by I. Beltrán-Hernández et al. presented a study on removing cadmium from aqueous solutions using a natural adsorbent like nopal (*Opuntia albicarpa* L. Scheinvar). The results presented suggested that using the thermally treated nopal (TN) achieved the best removal of cadmium (53.3%, corresponding to 0.155 mg g^{-1}) at pH 4.0.

The paper authored by Y. Ma et al. developed a colloidal gold immunochromatographic assay (GICA) for detecting immunodeficiency virus type 1 (HIV-1) p24 protein using mouse monoclonal antibodies (mAbs). The work presented achieved an overall specificity of 98.03% in the test and suggested that this method could be used as a convenient and efficient tool for early diagnosis of HIV infection.

Acknowledgments

We would like to thank all the authors for their excellent contributions to this special issue.

Weiqi Fu
Basel Khraiwesh
Hongbing Liu
Lei Kai

Hindawi Publishing Corporation
BioMed Research International
Volume 2016, Article ID 6743904, 6 pages
http://dx.doi.org/10.1155/2016/6743904

Research Article

Development of Monoclonal Antibodies against HIV-1 p24 Protein and Its Application in Colloidal Gold Immunochromatographic Assay for HIV-1 Detection

Yi Ma,[1] Chao Ni,[1] Emmanuel E. Dzakah,[1] Haiying Wang,[1] Keren Kang,[2] Shixing Tang,[2] Jihua Wang,[2] and Jufang Wang[1]

[1]*School of Bioscience and Bioengineering, South China University of Technology, Guangzhou 510006, China*
[2]*National Engineering Laboratory of Rapid Diagnostic Tests, Guangzhou Wondfo Biotech Co., Ltd., Guangzhou 510663, China*

Correspondence should be addressed to Jufang Wang; jufwang@scut.edu.cn

Received 10 December 2015; Accepted 15 February 2016

Academic Editor: Basel Khraiwesh

Human immunodeficiency virus type 1 (HIV-1) p24 protein is the most abundant viral protein of HIV-1. This protein is secreted in blood serum at high levels during the early stages of HIV-1 infection, making it a biomarker for early diagnosis. In this study, a colloidal gold immunochromatographic assay (GICA) was established for detecting p24 protein using mouse monoclonal antibodies (mAbs). The HIV-1 p24 protein was expressed in *E. coli* strain BL21 and the purified protein was used to immunize mice. Stable hybridoma cell lines secreting anti-p24 monoclonal antibodies were obtained after ELISA screening and subcloning by limiting dilution. 34 different capture and labeling mAb pairs were selected by a novel antibody-capture indirect sandwich ELISA and then applied in GICA to detect p24 protein. The GICA method has a limit of detection (LOD) of 25 pg/mL and could detect p24 protein in all 10 positive samples obtained from the National Reference of HIV-1 p24 antigen. Out of 153 negative samples tested, 3 false positives results were obtained. The overall specificity of this test was 98.03%. The good sensitivity and specificity of this method make it a suitable alternative to provide a more convenient and efficient tool for early diagnosis of HIV infection.

1. Introduction

P24 protein is derived from the Gag protein of HIV-1 and plays an important role in viral core assembly and maturation [1, 2]. HIV-1 RNA, anti-HIV antibodies, and p24 antigen are viral markers which have been used as a target antigen for early detection of HIV-1 infection [3, 4]. Over the past two decades, HIV immunoassays have gone through first-generation (using viral lysate for IgG antibody detection), second-generation (using recombinant antigens for IgG antibody detection), third-generation (IgM and IgG antibodies detection), and fourth-generation (antibody and p24 antigen detection) immunoassay. These test kits have helped to shorten the "window period" and provide an early diagnosis for suspected HIV infected samples as compared with the third-generation immunoassays.

Enzyme linked immunosorbent assay (ELISA) is the most commonly used immunoassay in the third- and fourth-generation test kits for HIV diagnosis in China. The limit of detection (LOD) for p24 antigen ranges from 11 pg/mL to 70 pg/mL [5]. However, ELISA involves complicated procedures and requires long reaction time of at least 2 hours. GICA has therefore been recognized as a popular diagnostic tool for the detection of HIV antibody because of its user-friendly format and easy and rapid rate of obtaining results without the need for special equipment [6–8]. There is no comprehensive study on p24 antigen detection using GICA and thus, the development of HIV-p24 antigen GICA, which can be used simultaneously with the HIV antibody GICA for rapid HIV detection, is of great significance. In this work, mAbs were screened against recombinant p24 protein and its application in GICA for HIV-1 detection was explored.

2. Materials and Methods

2.1. Strains, Plasmids, Enzymes, and Reagents. Competent *E. coli* cells DH5α and BL21 (DE3) were purchased from TIANGEN Biotech (Beijing, China). Restriction endonucleases *Nde*I and *Xho*I, Premix LA Taq, and DNA Ligation Kit were purchased from TAKARA Biotechnology Co., Ltd. (Dalian, China). SP2/0-Ag14 myeloma cells and pET-28a plasmid were preserved in our lab. All chemicals used in this study were of analytical grade.

2.2. Samples Collection and Examination. The National Reference of HIV-1 p24 antigen containing 10 positive samples (P1 to P10) and 10 sensitivity samples (L1 to L10) was purchased from the National Institute for the Control of Pharmaceutical and Biological Products (Beijing, China). These sensitivity samples were p24 protein (WHO standards) from the National Institute for Biological Standards and Control (Hertfordshire, UK) and diluted to concentrations of L1 (20 IU/mL), L2 (10 IU/mL), L3 (5 IU/mL), L4 (2.5 IU/mL), and L10 (0 IU/mL). Serum samples ($n = 153$) were collected from the General Hospital of Guangzhou Military Command of PLA. HIV antibody and p24 negative samples were confirmed by two different commercially available fourth-generation HIV ELISA test reagents.

2.3. Gene Cloning and Recombinant Protein Expression. DNA sequence of the 149~354-amino acid sequence of HIV p55 Gag protein in the NCBI database (NP_057850.1) encoding the p24 gene was designed with codon optimization and synthesized by Shanghai Shenggong Co., Ltd. (Shanghai, China). The purified p24 PCR product and the pET28a(+) plasmid were both double digested with *Nde*I and *Xho*I restriction enzymes and ligated by T4 DNA ligase to construct pET28a-p24 plasmid. *E. coli* BL21 (DE3) with recombinant plasmid were cultured in LB medium supplemented with 50 μg/mL kanamycin at 37°C until the logarithmic phase (at OD_{600} of 0.6~0.8) before induction with final concentration of 1.0 mM IPTG at 37°C, 25°C, and 18°C to OD_{600} of 2.0, respectively. Recombinant protein was purified on a HiTrap Ni^{2+} column using AKTAPurifier 100 (GE Healthcare Life Sciences, PA, USA).

2.4. Production of mAbs. Six-to-eight-week-old BALB/c mice were immunized subcutaneously with 100 μg r-p24 mixed with the equal volume of Freund's complete adjuvant (Sigma-Aldrich, MN, USA). On the 14th and 28th day, mice were boosted with 50 μg r-p24 mixed with the equal volume of Freund's incomplete adjuvant (Sigma-Aldrich, MN, USA). On day 38, a final injection of 50 μg r-p24 in PBS was administered intraperitoneally. Hybridoma and mAbs were generated as described previously [9].

2.5. Antibody-Capture Indirect Sandwich ELISA. A novel antibody-capture indirect sandwich ELISA method was designed to screen the mAb pairs recognizing r-p24. ELISA microtiter plates were coated with different mAbs (10 μg/mL in PBS, pH 9.6) and incubated overnight at 4°C followed by blocking with 3% BSA for 2 hr. For labeling of the detector antibody, 2 μg/mL of each mAb was dissolved in PBS dilution buffer (containing 0.05% (v/v) Tween 20 and 1% (v/v) BSA) and 0.1% (v/v) HRP conjugated goat-anti-mouse antibody (GAM-HRP) for 30 minutes before use. About 75 μL r-p24 (1 μg of protein/mL in PBS) containing 4% healthy mouse serum was incubated with 75 μL detector mAb for 5 mins reaction time after which 100 μL of the mixture was then added to each well in duplicate and then rinsed after 30 mins. The subsequent peroxidase reaction step was performed and all assay results were read with a microplate reader Thermo Scientific MK3 (Thermo Fisher Scientific, MA, USA) at wavelengths 450 nm.

2.6. Gold Immunochromatographic Assay for the Evaluation of p24 Protein. Monoclonal antibody pairs were used as capture and detector antibodies on the GICA platform. The detector antibody was labeled by conjugation to colloidal gold, mixed with active blocker against heterophilic antibodies and rheumatoid factor. The mixture was sprayed on glass fiber at 40 μL/cm^2. The capture mAb, goat-anti-mouse IgG, and active blocker were sprayed on a nitrocellulose membrane at a concentration of 2.0 mg/mL with a line thickness of 2 μL/cm to form the test, control, and block lines, respectively. Immunochromatographic test strips were made as described previously [10]. A maximum of 70 μL sample was added to the sample application site and the color development was observed after 20 mins.

2.7. GICA Test Strip Sensitivity to Recombinant p24 Antigen. Serial dilutions of r-p24 (1000 pg/mL, 250 pg/mL, 100 pg/mL, 50 pg/mL, 25 pg/mL, 10 pg/mL, and 0 pg/mL) were applied to the GICA test strips to check the sensitivity level at different antigen concentrations. Strips were observed for a maximum of 20 mins and the color development was compared with a standard color chart. The band intensity was then graded.

3. Results

3.1. Expression of Recombinant Protein. It was observed that higher incubation temperatures resulted in the formation of inclusion bodies while lower incubation temperatures showed high expression levels of soluble r-p24 proteins. The expression was carried out at 18°C and the r-p24 protein was purified on a HiTrap Ni^{2+} column with a total purity of >95% (Figure 1(a), lane 7). The purified protein of interest was confirmed by ELISA analysis of the protein using commercially available monoclonal antibody against p24 antigen (Figure 1(b)).

3.2. Screening of mAbs. 28 stable anti-r-p24 hybridoma clones were selected using indirect ELISA. Capture and detector mAb combinations were paired and selected from these 28 clones for reactivity against the immunogen through indirect sandwich ELISA. Of 784 (28×28) sandwich mAb combinations, 34 pairs could react with r-p24 at 1 μg/mL and 13 of those showed strong sensitivity with the r-p24 protein. A total of 15 mAbs pairs could react with 1 μg/mL r-p24 and only 2 mAbs pairs could react with 1 ng/mL r-p24. An

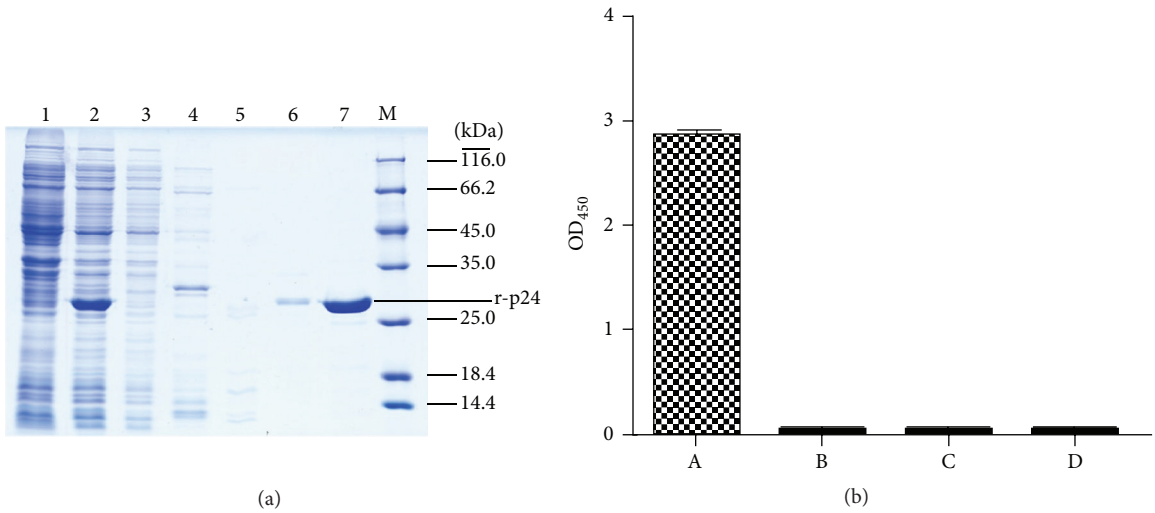

Figure 1: Preparation and identification of recombinant p24. (a) Expression and purification of recombinant p24. 1: whole cell lysate without IPTG induction, 2: whole cell lysate with IPTG induction, and 3: flow through solution; lanes 4 to 7 are four different solutions eluted by 50 mM, 150 mM, 300 mM, and 500 mM imidazole buffer, respectively. (b) Indirect ELISA analysis of the recombinant p24. A: antip24 antibody as the primary antibody, B: blank without primary antibody, C: blank without coating antigen, and D: blank without primary antibody and coating antigen.

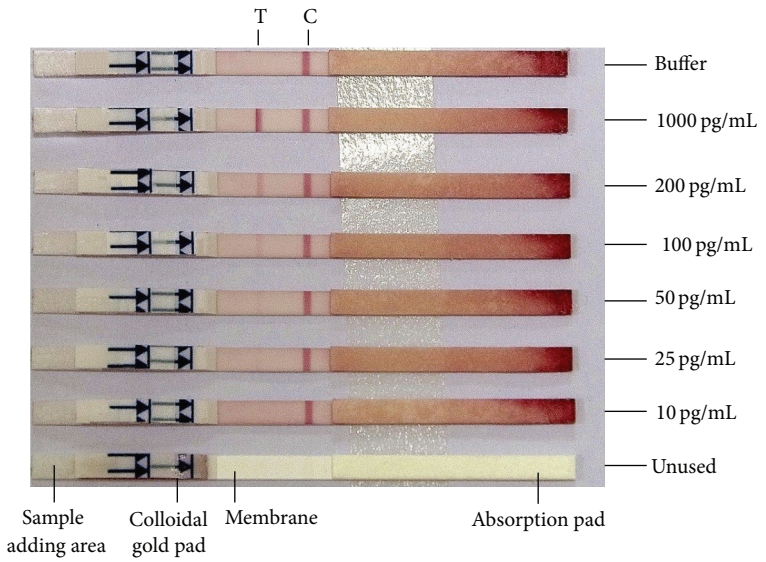

Figure 2: Sensitivity of GICA to r-p24 antigen. GICA test strips were treated with different concentrations (1000 pg/mL, 200 pg/mL, 100 pg/mL, 50 pg/mL, 25 pg/mL, and 10 pg/mL) of r-p24 antigen. T and C represent the test and control lines, respectively.

antibody pair consisting of capture (3-1D5) and detector (4-8A10) showed a relatively higher sensitivity to p24 and were selected for later GICA tests.

3.3. Test Strip Sensitivity to Recombinant p24 Antigen. The sensitivity of the test strips using capture (3-1D5) and detector (4-8A10) was determined by treatment with different antigen concentrations (1000 pg/mL, 200 pg/mL, 100 pg/mL, 50 pg/mL, 25 pg/mL, 10 pg/mL, and 0 pg/mL) and the band intensity was evaluated after 20 mins by comparing with a standard color chart. Desired sensitivity for GICA was observed at 25 pg/mL of antigen (Figure 2).

3.4. GICA for HIV-1 p24 Positive and Negative Samples. GICA lateral strips made of 3-1D5 and 4-8A10 were used to detect HIV-1 p24 antigen positive serum samples from the National Reference (NR) of HIV and p24 negative serum samples (Table 1). P1 to P10 (p24 positive samples in the NR) were consequently detected by the GICA method. Of the p24 sensitivity samples in the NR (L1 to L10), the L1, L2, and L3 samples with higher concentrations of p24 protein were positively detected by GICA while the lower concentration samples (L4–L10) were negative. Compared with the fourth-generation ELISA test reagent Vironostika HIV Uni-Form II Ag/Ab (Biomérieux, Boxtel, The Netherlands), three false

Table 1: The detection results of National Reference for HIV-1 p24 antigen by GICA strips.

Sample	Derivation of references	Genotype	Detection level
P1	P24 positive Sample 34#	AE	Faint
P2	P24 positive Sample 106#	B	Faint
P3	P24 positive Sample 116#	B	Medium
P4	P24 positive Sample 119#	B	Weak
P5	500 fold-diluted laboratory-grown virus sample A	Not given	Medium
P6	100 fold-diluted laboratory-grown virus sample A	Not given	Weak
P7	1000 fold-diluted laboratory-grown virus sample L	B	Faint
P8	10000 fold-diluted laboratory-grown virus sample L	B	Faint
P9	50 fold-diluted HIV-1 window period Sample P	AE	Faint
P10	WHO Standard p24 25 U/mL	B	Medium
L1	WHO Standard p24 20 U/mL	B	Medium
L2	WHO Standard p24 10 U/mL	B	Weak
L3	WHO Standard p24 5 U/mL	B	Faint
L4	WHO Standard p24 2.5 U/mL	B	Negative
L10	Buffer for L Series	B	Negative

Detection level: Band intensity was read independently by two individuals.

positives were observed in the GICA test when p24 negative serum samples ($n = 153$) were tested, giving an overall specificity of 98.03%.

4. Discussion

The number of new HIV infection cases has been on the increase despite numerous awareness programs and efforts to curtail the spread of infection. With the introduction of rapid HIV antibody test kits, HIV screening has become more decentralized with more tests done on an individual rather than batch [21]. Hence, there is an urgent need for simple, inexpensive, rapid, and accurate detection formats to shorten the window period of HIV testing and thereby reduce the risk of transmitting the virus from person to person during blood transfusion. GICA techniques have been applied in the third-generation HIV rapid detection reagents, but there are no commercialized available GICA rapid diagnostic reagents which can quickly detect HIV antibodies and HIV-1 p24 antigen in clinical samples. The development of rapid HIV testing reagents for p24 antigen detection could provide an easy detection method and would further enhance the sensitivity of currently available rapid test kits for early detection of HIV infection; hence, the production of HIV-1 p24 rapid GICA detection reagent is of great significance.

The GICA method described here could provide a much easier, rapid, and relatively inexpensive alternative to current ELISA protocols for p24 antigen detection. The LOD of 25 pg/mL for p24 is close to that observed in many commercially available antigen/antibody combination ELISAs. The GICA also demonstrated a good ability to detect low p24 concentrations in the National Reference of HIV-1 p24 antigen. This assay could detect all the 10 HIV-1 p24 positive serum samples including HIV-1 AE and B genotype samples. The sensitivity of the GICA was confirmed to be 5 IU/mL when WHO standard p24 sensitivity samples in the National Reference of HIV-1 p24 antigen were tested.

Chemiluminescent microparticle immunoassays and enzyme linked fluorescence assays have also been developed recently for commercial use, but these require complete packages of reagents and supports (Table 2). In the past decade, HIV-1 p24 antigen assays have significantly improved, as well as the introduction of new methodology such as nanoparticle-based biobarcode amplification assays, magnetic immunochromatography assays, and immunosensor assays (Table 2). It has also been reported that the ultrasensitive capacitive immunosensor assay can decrease the LOD of p24 antigen detection to about 7.9×10^{-8} pg/mL (Table 2). However, these assays generally require complex instruments or well-trained technicians for their operation which ultimately limit their use in point-of-care testing, especially in remote areas of most developing countries.

In this research, a novel antibody-capture indirect sandwich ELISA method was used for the rapid screening of antibody pairs. The selected antibody pairs showed good performance when applied in both sandwich ELISA and GICA. A total of 28 mAbs were obtained for combination experiments to screen the mAb pairs that could function well on GICA platform. Among these pairs, only one antibody pair showed the expected sensitivity for use on the GICA platform. Nevertheless, it is anticipated that more sensitive antibody pairs could be obtained by optimizing the immunization and antibody preparation process so as to enhance the sensitivity and specificity of the GICA kits. Most GICA mAb pairs perform well on the ELISA platform and some other immunological assays such as chemiluminescence microparticle immunoassay and fluorescence labeled immunochromatography. GICA strips can be applied in qualitative detection or semiquantitative detection of antigens. These results showed that the mAb pair can detect 20 pg/mL p24 antigen in ELISA method with HRP system (data not shown). In addition, fluorescent secondary antibody instead of colloidal gold can be used [22], and the consequent signal can be detected accurately by machine for p24 quantification.

Table 2: Comparison of GICA with some published HIV-1 p24 assays in recent years.

Assay	Support	p24 detection limit	Execution time
Colloidal gold immunochromatographic assay (GICA) Commercial assays	Lateral flow test strip	25 pg/mL	20 min
Abbott ARCHITECT HIV Ag/Ab Combo (Chemiluminescentmicroparticle immunoassay)	ARCHITECT automated analyzer	18.4 pg/mL (SFTS standard)	26 min [11]
Roche Elecsys® HIV combi (Chemiluminescentmicroparticle immunoassay)	Modular automated analyzer	0.9 IU/mL (WHO standard)	18 min [12]
Biomérieux VIDAS HIV DUO Ultra (Enzyme linked fluorescence assay)	VIDAS automated analyzer	11.5 pg/mL (SFTS standard)	120 min [13]
Bio-Rad GS HIV Combo Ag/Ab (Enzyme linked immunosorbent assay)	Bio-Rad EVOLIS™ Automated System	12.7 pg/mL (SFTS standard)	>120 min [14]
Bio-Rad Genscreen™ ULTRA HIV Ag-Ab (Enzyme linked immunosorbent assay)	Microplate	13 pg/mL (SFTS standard)	120 min [13]
Laboratory assays			
Ultrasensitive capacitive immunosensor assay	Capacitive immunosensor system	7.9×10^{-8} pg/mL	20 min [15]
Amperometricimmunosensor assay based on direct gold electroplating-modified electrode	Amperometricimmunosensor system	8 pg/mL	20 min [16]
Amperometricimmunosensor assay based on acetone-extracted propolis	Amperometricimmunosensor system	6.4 pg/mL	10 min [17]
Boosted ELISA based on immune complex dissociation and amplified signal	Microplate	0.5 pg/mL	>120 min [18]
Nanoparticle-based biobarcode amplification assay	NanosphereVerigene ID Reader	0.1 pg/mL	>120 min [19]
Magnetic immuno-chromatography assay	MagnaBiosciences magnetic assay reader	30 pg/mL	40 min [20]

SFTS standard: French national reference of HIV-1 p24 Ag obtained from the French Society of Blood Transfusion.

A rapid assay for the simultaneous detection of both p24 antigen and HIV specific antibody would provide a rapid diagnostic tool for screening HIV infected blood or serum specimen and may serve as a better substitute in commercially available fourth-generation ELISAs. Further researches could focus on improving the sensitivity and specificity of the GICA in detecting p24 antigen and HIV antibodies in a single device and thus accelerate their application in the fourth-generation HIV immunoassays.

Conflict of Interests

The authors declare that there is no conflict of interests regarding the publication of this paper.

Acknowledgments

This work was supported by the Science and Technology Planning Project of Guangdong Province (Grant no. 2012A080800007), the National Natural Science Foundation of China (Grant no. 21306055), Guangdong Natural Science Foundation (Grant no. 2014A030313261), and the Fundamental Research Funds for the Central Universities (Grant no. 2015ZM161).

References

[1] C. Momany, L. C. Kovari, A. J. Prongay et al., "Crystal structure of dimeric HIV-1 capsid protein," *Nature Structural Biology*, vol. 3, no. 9, pp. 763–770, 1996.

[2] M. F. Summers, L. E. Henderson, M. R. Chance et al., "Nucleocapsid zinc fingers detected in retroviruses: EXAFS studies of intact viruses and the solution-state structure of the nucleocapsid protein from HIV-1," *Protein Science*, vol. 1, no. 5, pp. 563–574, 1992.

[3] E. W. Fiebig, D. J. Wright, B. D. Rawal et al., "Dynamics of HIV viremia and antibody seroconversion in plasma donors: implications for diagnosis and staging of primary HIV infection," *AIDS*, vol. 17, no. 13, pp. 1871–1879, 2003.

[4] L. R. Petersen, G. A. Satten, R. Dodd et al., "Duration of time from onset of human immunodeficiency virus type 1 infectiousness to development of detectable antibody," *Transfusion*, vol. 34, no. 4, pp. 283–289, 1994.

[5] M. Miedouge, M. Grèze, A. Bailly, and J. Izopet, "Analytical sensitivity of four HIV combined antigen/antibody assays using the p24 WHO standard," *Journal of Clinical Virology*, vol. 50, no. 1, pp. 57–60, 2011.

[6] L.-R. Lin, Z.-G. Fu, B. Dan et al., "Development of a colloidal gold-immunochromatography assay to detect immunoglobulin G antibodies to *Treponema pallidum* with TPN17 and TPN47," *Diagnostic Microbiology and Infectious Disease*, vol. 68, no. 3, pp. 193–200, 2010.

[7] L. R. da Motta, A. C. Vanni, S. K. Kato et al., "Evaluation of five simple rapid HIV assays for potential use in the Brazilian national HIV testing algorithm," *Journal of Virological Methods*, vol. 194, no. 1-2, pp. 132–137, 2013.

[8] G. P. Zhang, X. N. Wang, J. F. Yang et al., "Development of an immunochromatographic lateral flow test strip for detection of β-adrenergic agonist *Clenbuterol residues*," *Journal of Immunological Methods*, vol. 312, no. 1-2, pp. 27–33, 2006.

[9] E. E. Dzakah, K. Kang, C. Ni et al., "Plasmodium vivax aldolase-specific monoclonal antibodies and its application in clinical diagnosis of malaria infections in China," *Malaria Journal*, vol. 12, no. 1, pp. 199–206, 2013.

[10] A. Fatima, H. Wang, K. Kang et al., "Development of VHH antibodies against dengue virus type 2 NS1 and comparison with monoclonal antibodies for use in immunological diagnosis," *PLoS ONE*, vol. 9, no. 4, Article ID e95263, 2014.

[11] C. A. Brennan, J. Yamaguchi, A. Vallari, P. Swanson, and J. R. Hackett, "ARCHITECT® HIV Ag/Ab Combo assay: correlation of HIV-1 p24 antigen sensitivity and RNA viral load using genetically diverse virus isolates," *Journal of Clinical Virology*, vol. 57, no. 2, pp. 169–172, 2013.

[12] C. M. Tao, Y. Cho, K. P. Ng et al., "Validation of the Elecsys® HIV combi PT assay for screening and reliable early detection of HIV-1 infection in Asia," *Journal of Clinical Virology*, vol. 58, no. 1, pp. 221–226, 2013.

[13] T. D. Ly, A. Ebel, V. Faucher, V. Fihman, and S. Laperche, "Could the new HIV combined p24 antigen and antibody assays replace p24 antigen specific assays?" *Journal of Virological Methods*, vol. 143, no. 1, pp. 86–94, 2007.

[14] E. O. Mitchell, G. Stewart, O. Bajzik, M. Ferret, C. Bentsen, and M. K. Shriver, "Performance comparison of the 4th generation Bio-Rad Laboratories GS HIV Combo Ag/Ab EIA on the EVOLIS™ automated system versus Abbott ARCHITECT HIV Ag/Ab Combo, Ortho Anti-HIV 1 + 2 EIA on Vitros ECi and Siemens HIV-1/O/2 enhanced on Advia Centaur," *Journal of Clinical Virology*, vol. 58, supplement 1, pp. e79–e84, 2013.

[15] K. Teeparuksapun, M. Hedström, E. Y. Wong, S. Tang, I. K. Hewlett, and B. Mattiasson, "Ultrasensitive detection of HIV-1 p24 antigen using nanofunctionalized surfaces in a capacitive immunosensor," *Analytical Chemistry*, vol. 82, no. 20, pp. 8406–8411, 2010.

[16] L. Zheng, L. Jia, B. Li et al., "A sandwich HIV p24 amperometric immunosensor based on a direct gold electroplating-modified electrode," *Molecules*, vol. 17, no. 5, pp. 5988–6000, 2012.

[17] F. Kheiri, R. E. Sabzi, E. Jannatdoust, E. Shojaeefar, and H. Sedghi, "A novel amperometric immunosensor based on acetone-extracted propolis for the detection of the HIV-1 p24 antigen," *Biosensors and Bioelectronics*, vol. 26, no. 11, pp. 4457–4463, 2011.

[18] R. Sutthent, N. Gaudart, K. Chokpaibulkit, N. Tanliang, C. Kanoksinsombath, and P. Chaisilwatana, "p24 antigen detection assay modified with a booster step for diagnosis and monitoring of human immunodeficiency virus type 1 infection," *Journal of Clinical Microbiology*, vol. 41, no. 3, pp. 1016–1022, 2003.

[19] S. Tang, J. Zhao, J. J. Storhoff et al., "Nanoparticle-based biobarcode amplification assay (BCA) for sensitive and early detection of human immunodeficiency type 1 capsid (p24) antigen," *Journal of Acquired Immune Deficiency Syndromes*, vol. 46, no. 2, pp. 231–237, 2007.

[20] S. Workman, S. K. Wells, C.-P. Pau et al., "Rapid detection of HIV-1 p24 antigen using magnetic immuno-chromatography (MICT)," *Journal of Virological Methods*, vol. 160, no. 1-2, pp. 14–21, 2009.

[21] T. C. Granade, "Use of rapid HIV antibody testing for controlling the HIV pandemic," *Expert Review of Anti-infective Therapy*, vol. 3, no. 6, pp. 957–969, 2005.

[22] Z. Bai, Y. Luo, W. Xu et al., "Development of a new fluorescence immunochromatography strip for detection of chloramphenicol residues in chicken muscles," *Journal of the Science of Food and Agriculture*, vol. 93, no. 15, pp. 3743–3747, 2013.

Hindawi Publishing Corporation
BioMed Research International
Volume 2016, Article ID 1423828, 8 pages
http://dx.doi.org/10.1155/2016/1423828

Research Article

Biochemical and Metabolic Changes in Arsenic Contaminated *Boehmeria nivea* L.

Hussani Mubarak,[1,2] Nosheen Mirza,[1,2,3] Li-Yuan Chai,[1,2] Zhi-Hui Yang,[1,2] Wang Yong,[1,2] Chong-Jian Tang,[1,2] Qaisar Mahmood,[3] Arshid Pervez,[3] Umar Farooq,[4] Shah Fahad,[5] Wajid Nasim,[6] and Kadambot H. M. Siddique[7]

[1]*Department of Environmental Engineering, School of Metallurgy and Environment, Central South University, Changsha, Hunan 410083, China*
[2]*National Engineering Research Center for Control and Treatment of Heavy Metal Pollution, Changsha 410083, China*
[3]*Department of Environmental Sciences, COMSATS Institute of Information Technology, Abbottabad 22060, Pakistan*
[4]*Department of Chemistry, COMSATS Institute of Information Technology, Abbottabad 22060, Pakistan*
[5]*College of Plant Science and Technology, Huazhong Agricultural University, Wuhan, Hubei 430070, China*
[6]*Department of Environmental Sciences, COMSATS Institute of Information Technology (CIIT), Vehari, Pakistan*
[7]*The UWA Institute of Agriculture, The University of Western Australia, Perth, WA 6009, Australia*

Correspondence should be addressed to Zhi-Hui Yang; yangzh@csu.edu.cn

Received 19 November 2015; Revised 5 February 2016; Accepted 8 February 2016

Academic Editor: Hongbing Liu

Arsenic (As) is identified by the EPA as the third highest toxic inorganic contaminant. Almost every 9th or 10th human in more than 70 countries including mainland China is affected by As. Arsenic along with other toxins not only affects human life but also creates alarming situations such as the deterioration of farm lands and desertion of industrial/mining lands. Researchers and administrators have agreed to opt for phytoremediation of As over costly cleanups. *Boehmeria nivea* L. can soak up various heavy metals, such as Sb, Cd, Pb, and Zn. But the effect of As pollution on the biology and metabolism of *B. nivea* has been somewhat overlooked. This study attempts to evaluate the extent of As resistance, chlorophyll content, and metabolic changes in As-polluted (5, 10, 15, and 20 mg L^{-1} As) *B. nivea* in hydroponics. Toxic effects of As in the form of inhibited growth were apparent at the highest level of added As. The significant changes in the chlorophyll, electrolyte leakage, and H_2O_2, significant increases in As in plant parts, catalase (CAT), and malondialdehyde (MDA), with applied As revealed the potential of *B. nivea* for As decontamination. By employing the metabolic machinery of *B. nivea*, As was sustainably removed from the contaminated areas.

1. Introduction

Ramie (*Boehmeria nivea*), commonly known as China grass, is an important fiber crop which has been widely cultivated and distributed in China. It is a perennial plant with at least three harvests per year [1]. The principal end product of *B. nivea* is textile grade fiber, famous for its fine characteristics in textile industries [2]. The leaf and the root extracts of the plant have antimicrobial, anti-inflammatory, antioxidant, and hepatoprotective properties [3]. Ramie grows in the wild and is known to colonize both active and abandoned metal mine sites. It is capable of accumulating certain amounts of toxins such as Sb, Cd, and Hg [4, 5]. Other studies have shown that ramie can also tolerate certain amounts of heavy metals such as mercury, lead [6], cadmium [7, 8], and arsenic [1].

Across the globe, centuries of unsustainable activities have resulted in severe heavy metal contamination which has damaged aquatic and terrestrial environments [9]. Arsenic (As) is one of these reported toxins and is carcinogenic. It is a ubiquitous element and its toxicity in the environment is a global issue. The increasing As contamination in water, soils, and crops in numerous countries such as India, Bangladesh, Cambodia, Laos, Myanmar, China, Taiwan, United States, Vietnam, Thailand, and Europe is well reported [9, 10]. The

health problems associated with chronic exposure to As are diabetes, cancer, poisoning, pathogenic potential of bacteria or fecal coliform, and blood stream infections. In China, high arsenic groundwater has been observed in the Datong basin of Shanxi Province, Hetao basin of Inner Mongolia, Xinjiang and Taiwan Provinces. In these regions, approximately 18.5 million people are at risk of exposure to high arsenic groundwater [11].

Colonization of *B. nivea* and accumulation of heavy metals such as Sb, Cd, Pb, and Zn in metal-contaminated regions have been reported. *B. nivea* has a high tolerance to As contamination [12]. The effect of As pollution on the biology of *B. nivea*, the potential tolerance of *B. nivea* to As pollution, and the metabolic changes in *B. nivea* under the reported ranges of As contamination has not been documented. Based on the above review [12], the objectives of the current study were to evaluate plant growth, metabolic changes, and the ability of *B. nivea* L. to uptake and accumulate As in an attempt to determine the effects of As on chlorophyll content, antioxidative systems, and lipid membrane peroxidation in order to better understand the cellular basis of As tolerance in *B. nivea*.

2. Materials and Methods

2.1. Plant Materials and Growth Conditions. Young shoot cuttings (14 cm) of *B. nivea* plants were collected from an active and abandoned mining area in Xikuangshan, Hunan Province, China (29°N, 120°E). The cuttings were planted in sand for root initiation and then transferred to 1/2 strength Hoagland solution until they reached a height of 30 cm (40 days).

2.2. Hydroponic Experiment. After 40 days, the plants were transferred to 1/2 strength Hoagland solution (2 L) spiked with 0, 5, 10, 15, or 20 mg L^{-1} of arsenic. Arsenic (As) was applied as $NaAsO_2$ (As-III, 100% purity). Each treatment was replicated three times. After 14 days of As exposure, the roots were immersed in 20 mM Na_2-EDTA for 30 min to remove the As adsorbed to the roots, and the entire plant was rinsed three times with deionized water. The roots, stems, and leaves were separated. For further analysis, some of the fresh top leaves were frozen at −80°C and some were dried at 70°C. The remaining Hoagland solution was filtered and refrigerated for later As analysis. The stress tolerance index of As-contaminated *B. nivea* was calculated according to Yang et al. and Ismail et al. [1, 13].

The stress tolerance index (%) was calculated using the following formula:

$$\text{Stress tolerance index} = \frac{\text{Shoot length of stress plant}}{\text{Shoot length of control plant}} \times 100. \quad (1)$$

2.3. Metabolism of B. nivea

2.3.1. Chlorophyll Analysis. The 6th fully expanded leaf from the top of each plant was used to measure chlorophyll a, chlorophyll b, and total chlorophyll (chl (a + b)). Chlorophyll a, chlorophyll b, and chl (a + b) were analyzed according to the methods of Arnon and Huang et al. [14, 15] and estimated using the formulas of Ehsan et al. and Metzner et al. [16, 17]:

$$\begin{aligned} &\text{Chlorophyll a } \left(\mu\text{g mL}^{-1}\right) \\ &\quad = 10.3 \times E663 - 0.98 \times E644 \\ &\text{Chlorophyll b } \left(\mu\text{g mL}^{-1}\right) \\ &\quad = 19.7 \times E644 - 3.87 \times E663 \\ &\text{Total chlorophyll} = \text{Chlorophyll a} + \text{Chlorophyll b}. \end{aligned} \quad (2)$$

2.3.2. Assessment of Antioxidants. Physiological measurements were performed on the 5th leaf from the top of plants growing in well-watered As conditions. Approximately 0.2 g of fresh tissue was homogenized in a precooled mortar with 5 mL of 50 mmol L^{-1} precooled phosphate buffer (pH 7.8). The homogenate was centrifuged at 11,000 g for 20 min at 4°C. The supernatant (i.e., the enzyme extract) was used to determine enzyme activities—superoxide dismutase (SOD), peroxidase (POD), catalase (CAT), and malondialdehyde content (MDA) [18, 19].

2.3.3. Assessment of Electrolyte Leakage and Hydrogen Peroxide Levels. Electrolyte leakages in 5 mm long fragments of fully expanded leaves were determined. The fragment tubes were incubated in a water bath at 32°C for 2 hours with the initial electrical conductivity (EC) of the medium, EC_1, noted. The samples were autoclaved at 121°C for 20 min to discharge the electrolytes and then cooled to 25°C. The final EC_2 was measured [20, 21]. Electrolyte leakage (EL) was calculated using the following formula:

$$\text{EL} = \left(\frac{EC_1}{EC_2}\right) \times 100. \quad (3)$$

H_2O_2 contents were assayed colorimetrically as documented by Jana and Choudhuri and Shakoor et al. [22, 23]. The hydrogen peroxide was extracted by homogenizing 0.05 g leaf tissues with 3 mL of phosphate buffer (50 mM, pH 6.5). The homogenate was centrifuged at 6,000 g for 25 min. To measure H_2O_2 content, 2.5 mL of the extracted solution was mixed with 1 mL of 0.1% titanium sulfate ($Ti(SO_4)_2$) in 20% (v/v) H_2SO_4. The mixture was centrifuged at 6,000 g for 15 min. The intensity of the yellow color supernatant was analyzed at 410 nm. The H_2O_2 content was calculated by applying an extinction coefficient of 0.28 $mmol^{-1}$ cm^{-1}.

2.3.4. Assessment of Relative Water Contents (RWC). The RWC was determined using the methods of Huang et al. and Yamasaki and Dillenburg [15, 24]. The fresh mass (FM) of leaves was immersed in distilled water for 12 h to determine turgid mass (TM). Leaves were then dried at 70°C for 48 h to determinate dry mass (DM). The RWC was calculated as follows:

$$\text{RWC} = \left[\frac{(\text{FM} - \text{DM})}{(\text{TM} - \text{DM})}\right] \times 100. \quad (4)$$

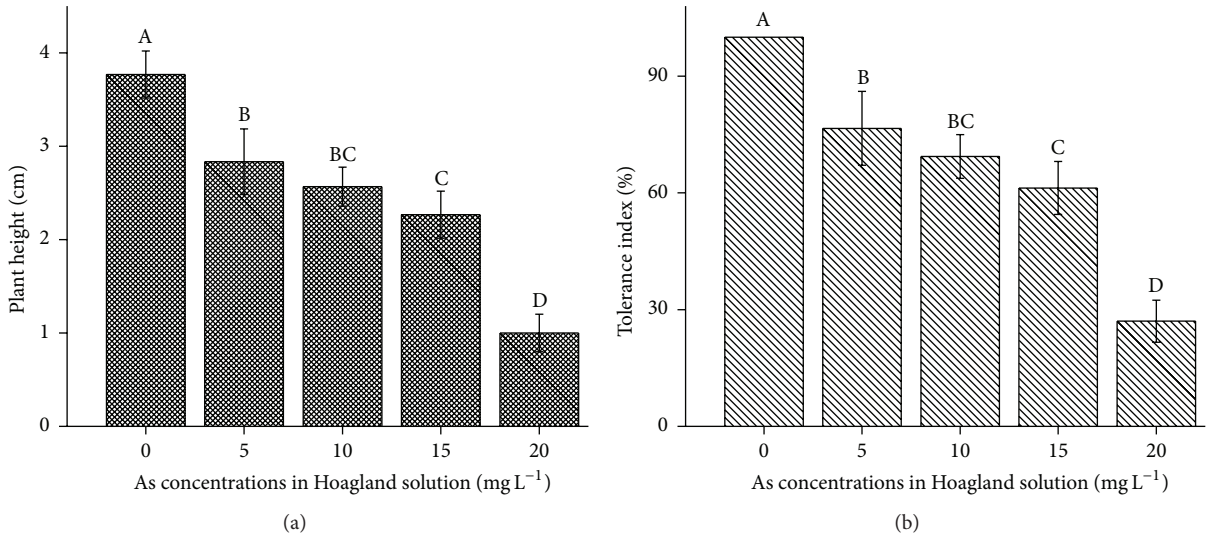

Figure 1: (a) Effect of As application, on the height of *Boehmeria nivea* L. (b) Effect of As application, on the tolerance index of *Boehmeria nivea*. Values followed by different uppercase letters are significantly different at $P < 0.05$, for treatments. Different letters indicate significant differences between treatments for each parameter, at significant level of 0.05. Values followed by the same letters for each parameter are not significantly different at the 0.05 level (least significant difference). Values in the graph are mean ($n = 3$); error bars are standard deviation (SD).

2.4. Arsenic (As) Analysis. The dried plant samples were ground, sieved (1 mm), and digested with $HNO_3 : HClO_4$ (4 : 1, v/v). The As concentration in plant parts was analyzed using Induced Couple Plasma-Optical Emission Spectrometer (ICP-OES) (Perkin Elmer, Precisely, Shelton, CT 06484, USA, Optima™ 5300 DV Spectrometer). For accuracy of the digestion and analytical method, a blank sample (4 mL HNO_3 + 1 mL $HClO_4$) was also run with the samples.

2.5. Data Analysis. Analysis of variance (ANOVA) at a significance level of $P < 0.05$ was performed using the General Linear Model (GLM) in the SAS package. The LSD test and t-test were employed to compare significant differences between means for the treatments at $P < 0.05$. The results are expressed as means ± SD. Graphical analyses were carried out using Origin Pro 8.5.

3. Results and Discussion

3.1. Growth of B. nivea. Field surveys have reported the presence of healthy growing *B. nivea* plants in toxic metal-contaminated areas [8, 25], but only a few studies have reported As resistance in *B. nivea*. The higher tolerance of *B. nivea*, compared to other plant species, for toxic [26] and heavy metals [27], has been estimated and documented. The metabolic responses of *B. nivea* under specific As ranges, say between 10 and 250 mg kg^{-1} soil, have not been assessed.

The As-contamination (hydroponic) treatments inhibited the growth of *B. nivea* more so as the contamination increased (Figure 1(a)). Plant height decreased with increasing As concentration. At 0 mg L^{-1} As, plant height ranged from 3.8 to 4 cm; the As treatments at 5, 10, 15, and 20 mg L^{-1} reduced plant height by 25, 32, 40, and 73% of the control, respectively. The As tolerance index of *B. nivea* significantly decreased ($P < 0.05$) as As concentration increased (Figure 1(b)) and ranged from 27 to 77%.

3.2. Metabolism of As-Contaminated B. nivea L.

3.2.1. Chlorophyll Content of B. nivea L. The effect of applied As on chlorophyll content is presented in Figure 2. As the As concentration increased, all chlorophyll content measurements (chl a, chl b, and chl a + b) significantly decreased ($P < 0.05$) in *B. nivea* by 11–54%, 22–54% and 14–54%, respectively, relative to the control (Figure 2). Singh et al. [28] reported increased chlorophyll contents in *Pteris vittata* but decreased chlorophyll contents in *Pteris ensiformis* under As-induced stress.

3.2.2. Activities of Antioxidant Enzymes in B. nivea L. Increasing As concentration had a significant ($P < 0.05$) effect on SOD, CAT, and MDA concentrations in *B. nivea* (Figures 3(a)–3(d)). Compared with the control, increasing the As concentration significantly decreased ($P < 0.05$) SOD concentration in *B. nivea*, except at the highest applied As (20 mg L^{-1}), while there were a nonsignificant reduction in POD concentration and a gradual reduction in CAT concentration at 10 mg L^{-1}, but a slight increase at 15 and 20 mg L^{-1}. The MDA content in As-contaminated *B. nivea* showed a significant ($P < 0.05$) increasing trend with increasing As concentration.

In plants and living organisms, stress induces the generation of reactive oxygen species (ROS) which may cause oxidative damage to proteins and enzymes. Excessive ROS increases MDA, the last product of membrane liposome peroxidation, which suggests lipid membrane instability [29].

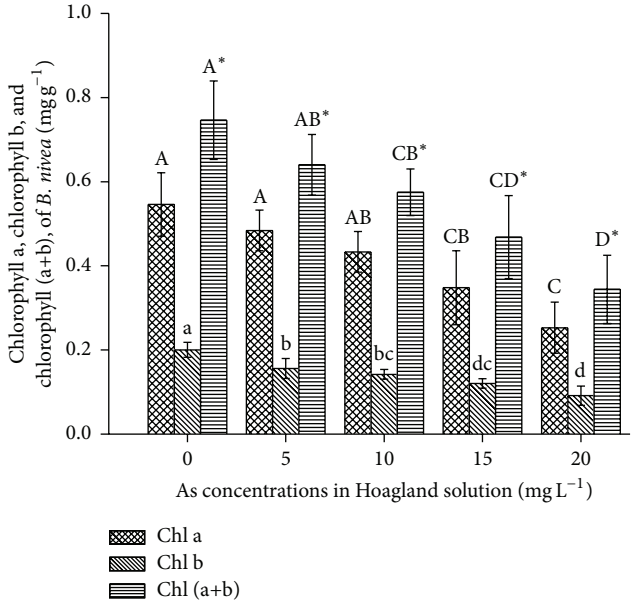

FIGURE 2: Effect of As application, on the chlorophyll of *Boehmeria nivea* L. Values followed by different uppercase letters are significantly different at $P < 0.05$, for treatments. Values followed by different lowercase letters are significantly different at $P < 0.05$, for treatments. Values followed by different uppercase letters* are significantly different at $P < 0.05$, for treatments. Different letters indicate significant differences between treatments for each parameter, at significant level of 0.05. Values followed by the same letters for each parameter are not significantly different at the 0.05 level (least significant difference). Values in the graph are mean ($n = 3$); error bars are standard deviation (SD).

To reduce oxidative damage, plants initiate enzymatic and nonenzymatic antioxidant defense mechanisms, of which the synthesis of SOD, POD, and CAT is the most important. In *B. nivea*, the greatest increase in MDA, relative to the control, was at 20 mg L^{-1} As (Figures 3(a)–3(c)), demonstrating that POD and CAT are H_2O_2 scavengers in ramie. SOD, POD, and CAT activities had similar suppressive effects and enhanced trends with As addition, except for POD concentration at 10 mg L^{-1} As and CAT at 15 mg L^{-1} As. The critical-stage performance of antioxidants, in *B. nivea*, was at 20 mg L^{-1} As.

SOD contents in *B. nivea* decreased by approximately 1.2, 1.5, 2.0, and 1 times of the control at 5, 10, 15, and 20 mg L^{-1} As, respectively (Figure 3(a)). Based on this and the observed fluctuations, we conclude that SOD contributed to the tolerance of *B. nivea* to As contamination. At 5, 10, 15, and 20 mg L^{-1} As, POD content declined by approximately 1.1, 1.0, 1.2, and 1.0 times of the control, respectively (Figure 3(b)). Similar decreasing trends of SOD and POD contents in cadmium-stressed wheat (*Triticum durum*) and selenium-stressed ryegrass (*Lolium perenne*) have been reported [19]. A study by Saidi et al. [30] reported suppressed activities of SOD and POD in cadmium-contaminated bean plants, while Huang et al. [31] reported increased SOD and POD contents in hybrid ramie under increased salinity.

The CAT content in *B. nivea* decreased at 5, 10, 15, and 20 mg L^{-1} by 1.6-, 2.3-, 1.4-, and 1.1-fold less than control (Figure 3(c)). Silva et al. and Huang et al. [31, 32] reported decreasing CAT content in aluminum-exposed rye and salinity-stressed ramie. The decreased CAT activity with increasing As contamination confirms the role of CAT in quenching H_2O_2 and preventing oxidative damage in *B. nivea*.

Increasing the concentration of As in *B. nivea* increased MDA concentration from 1.12 times greater than control at 5 mg L^{-1} to 2.20 times greater than control at 20 mg L^{-1} (Figure 3(d)). The increase at 20 mg L^{-1} As suggests the role of MDA in lipid peroxidation and the maintenance of homeostasis of *B. nivea*. Increases in MDA activity below 20 mg L^{-1} As inhibited biomass production which is a clear indication of As tolerance of *B. nivea*. Our results of enhanced MDA and CAT activities with As addition agree with those of Feng et al. and Huang et al. [29, 31] who reported increased MDA and CAT activities in drought-stressed drought-resistant ramie cultivars, plants (ferns, rice, and maize) and hybrid ramie (*B. nivea*), respectively. Our results suggest that *B. nivea* is capable of alleviating oxidative stress and preventing lipid peroxidation under a specified range (5–15 mg L^{-1} As) of As contamination. The highest increase in MDA (2.20 times greater than control) at 20 mg L^{-1} confirms lipid peroxidation or damage to the plasma membrane which, in turn, inhibits plant growth.

3.2.3. Electrolyte Leakage and Hydrogen Peroxide (H_2O_2) Levels in B. nivea L. Solute leakage and H_2O_2 content increased in *B. nivea* with increasing As contamination (Figures 4(a) and 4(b)). The increases in electrolyte leakage and H_2O_2 from 5 to 20 mg L^{-1} As ranged from 1- to 1.5-fold and 1.13- to 2-fold greater than the control, respectively. The gradual increase in MDA, electrolyte leakage, and H_2O_2 from 5 to 15 mg L^{-1} As revealed that As toxicity accelerated the antioxidant defense mechanism [15]. However, 20 mg L^{-1} As resulted in oxidative destruction in the plant. Similar trends for electrolyte leakage and lipid peroxidation have been reported in Cu-, Cd-, and Pb-contaminated *Brassica napus* [16, 20, 23].

3.2.4. Relative Water Contents (RWC) in B. nivea L. As contamination reduced RWC in ramie, it was not significant ($P > 0.05$) (Figure 5). The reductions in RWC were 1.01–1.04-fold less than the control (1–4%) at 5–20 mg L^{-1} As. However, the greatest reduction in RWC (4%) was recorded at 20 mg L^{-1} As (Figure 5). The antioxidant defense mechanism enabled *B. nivea* to maintain tissue water potential and, therefore, cell turgor under the stress conditions [15]. Turgidity maintenance under stress leads to the maintenance of comparatively higher RWC under increasing As contamination (Figure 5). Similar trends for RWC and lipid peroxidation have been reported in Pb-contaminated ramie cultivars [15].

3.3. Arsenic (As) Concentration in B. nivea L. The As content in dried roots and shoots (leaves plus stem) of *B. nivea* increased significantly ($P < 0.05$) with increasing applied As (Figure 6), more so in the shoots than the roots. Arsenic (As) mostly accumulates in the aboveground parts of tolerant

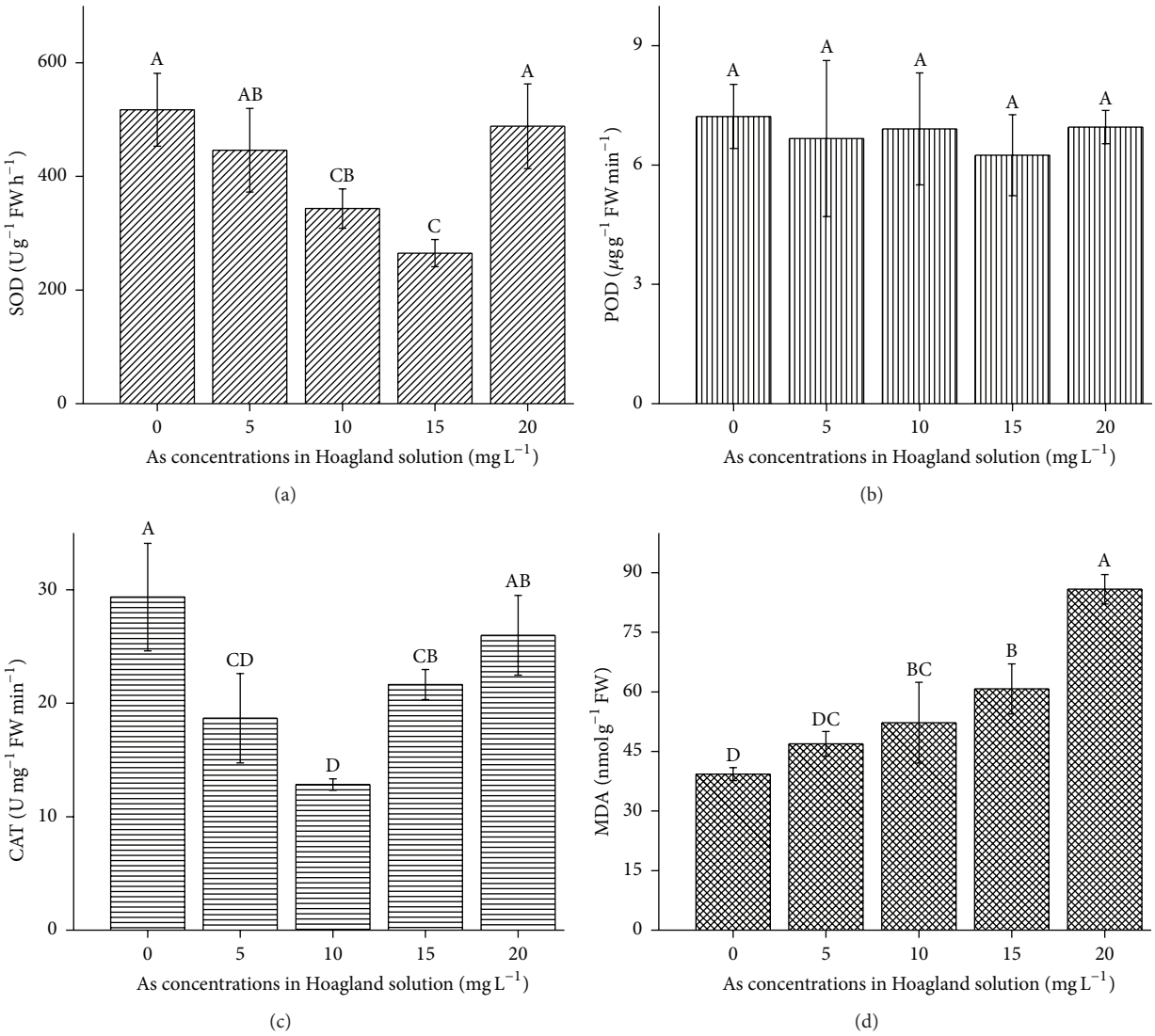

Figure 3: Effect of As application on antioxidant enzymes of *Boehmeria nivea*. (a): SOD; (b): POD; (c): CAT; (d): MDA. Values followed by different uppercase letters are significantly different at $P < 0.05$, for treatments. Different letters indicate significant differences between treatments for each parameter, at significant level of 0.05. Values followed by the same letters for each parameter are not significantly different at the 0.05 level (least significant difference). Values in the graph are mean ± SD ($n = 3$); error bars are SD.

plants. The average amount of As remaining in the Hoagland solution at the end of the experiment was 89%.

The concentrations of As in the shoots and roots of *B. nivea* gradually significantly increased within a certain range, that is, 330–150 mg kg^{-1}, respectively, compared to the control (94–75% > control). Shoot accumulation of As in *B. nivea* at 5 and 20 mg L^{-1} As was 4.0 and 15.5 times greater than the control, respectively, while in the roots the respective values were 8.0 and 17.0 times greater than the control, respectively. The average amount of As remaining in the Hoagland solution at 5, 10, 15, and 20 mg L^{-1} was 85, 86, 88, and 99% (i.e., 15, 14, 12, and 1% were absorbed by *B. nivea*), respectively. Thus, the performance of *B. nivea* improved with increasing addition of As. The mobilization of As from roots to leaves is the greatest threat to the food chain and the survival of life on Earth, but this would not occur in *B. nivea* because it annually sheds older leaves (which can be collected, removed, and/or recycled) and is a commercial fiber crop; hence, contamination of the food chain is avoided.

In contrast to our results, Otones et al. [33] recommended *Agrostis castellana* (Boiss. & Reut.), *Centaurea jacea* L., *Eryngium campestre* L., and *Scirpus holoschoenus* L. for the stabilization of As in abandoned mining areas. According to this study, these plants showed low translocation factors, that is, underground [As] > aboveground [As]. In accordance with our results *Helichrysum oligocephalum*, *Hyoscyamus kurdicus*, *Nonea persica*, *Salvia syriaca* [34], *Rumex acetosella* L. [33], *Arundo donax* [35], *Isatis cappadocica*, and *Hesperis persica* [36] reportedly accumulate relatively high As concentrations in their shoots.

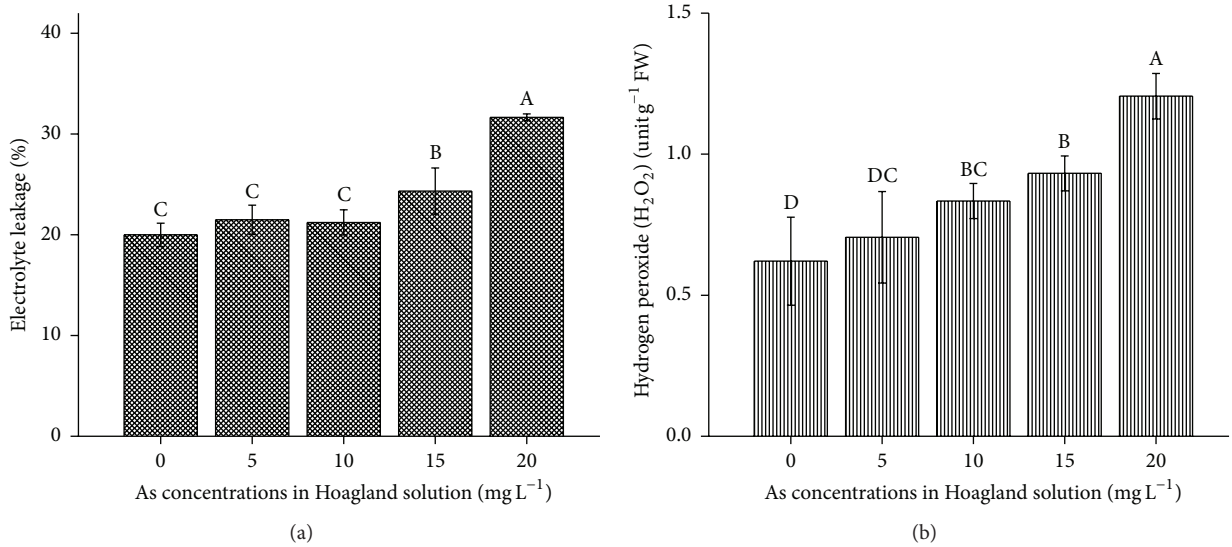

Figure 4: (a) Effect of As application, on the electrolyte leakage in *Boehmeria nivea* L. (b) Effect of As application, on the H_2O_2 in *Boehmeria nivea* L. Values followed by different uppercase letters are significantly different at $P < 0.05$, for treatments. Different letters indicate significant differences between treatments for each parameter, at significant level of 0.05. Values followed by the same letters for each parameter are not significantly different at the 0.05 level (least significant difference). Values in the graph are mean ($n = 3$); error bars are standard deviation (SD).

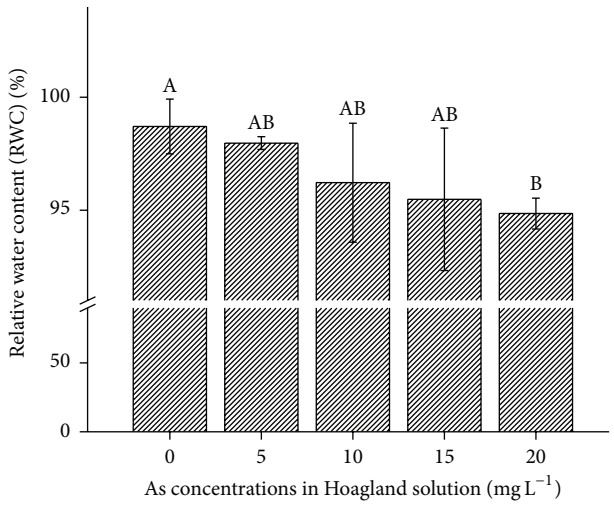

Figure 5: Effect of As application, on the RWC in *Boehmeria nivea* L. Values followed by different uppercase letters are significantly different at $P < 0.05$, for treatments. Different letters indicate significant differences between treatments for each parameter, at significant level of 0.05. Values followed by the same letters for each parameter are not significantly different at the 0.05 level (least significant difference). Values in the graph are mean ($n = 3$); error bars are standard deviation (SD).

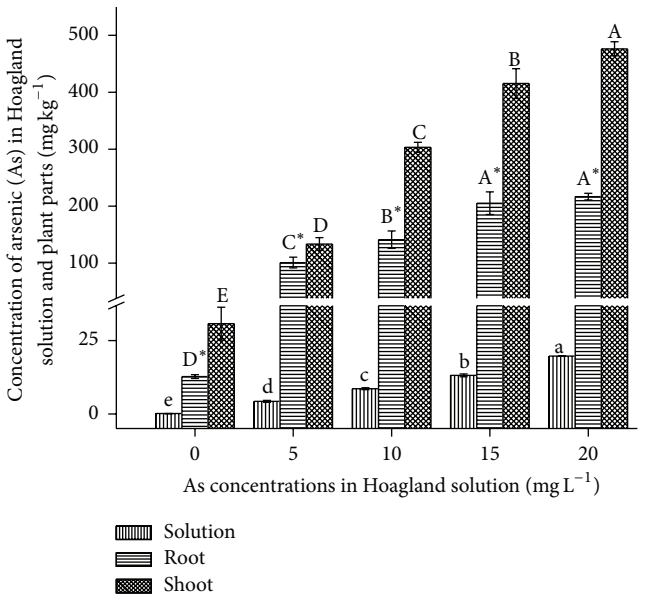

Figure 6: Effect of As application, on the As concentration in Hoagland solution and plant parts of *Boehmeria nivea* L. Values followed by different uppercase letters are significantly different at $P < 0.05$, for treatments. Values followed by different lowercase letters are significantly different at $P < 0.05$, for treatments. Values followed by different uppercase letters* are significantly different at $P < 0.05$, for treatments. Different letters indicate significant differences between treatments for each parameter, at significant level of 0.05. Values followed by the same letters for each parameter are not significantly different at the 0.05 level (least significant difference). Values in the graph are mean ($n = 3$); error bars are standard deviation (SD).

4. Conclusions

This study reports on the growth of *B. nivea* in As-contaminated hydroponic cultures up to 20 mg L^{-1}. Arsenic contamination at high concentration, that is, 20 mg L^{-1}, can inhibit

growth, chlorophyll content, and SOD, CAT, and POD contents in the plant by inducing electrolyte leakage, lipid peroxidation, and reducing RWC. However, up to 15 mg L^{-1} As resulted in limited cellular oxidative damage in *B. nivea*. The plant accumulated higher As concentrations in shoots than roots and thus gave higher translocation factors. The ability to accumulate more metals in the stalk and leaves than roots is a positive indicator. The metabolic and biochemical processes in *B nivea* remain unaffected till 15 mg L^{-1} As, but at 20 mg L^{-1} stress-induced oxidative damage was apparent. This experiment suggests that *B. nivea* L. may extract a considerable amount of As; however a field-based study is needed to confirm these results.

Conflict of Interests

The authors declare that there is no conflict of interests regarding the publication of this paper.

Acknowledgments

The financial support of this work by the Science and Technology Program for Public Wellbeing (2012GS430201) and the Key Project of Science and Technology of Hunan Province, China (2012FJ1010), is gratefully acknowledged.

References

[1] B. Yang, M. Zhou, W. S. Shu et al., "Constitutional tolerance to heavy metals of a fiber crop, ramie (*Boehmeria nivea*), and its potential usage," *Environmental Pollution*, vol. 158, no. 2, pp. 551–558, 2010.

[2] R. Kozlowaski, M. Rawluk, and J. Barriga-Bedoya, "Ramie," in *Bast and Leaf Fibre Crops*, R. R. Frank, Ed., pp. 207–227, Woodhead Publishing, Cambridge, UK; CRC Press, New York, NY, USA, 2005.

[3] K.-L. Huang, Y.-K. Lai, C.-C. Lin, and J.-M. Chang, "Involvement of GRP78 in inhibition of HBV secretion by *Boehmeria nivea* extract in human HepG2 2.2.15 cells," *Journal of Viral Hepatitis*, vol. 16, no. 5, pp. 367–375, 2009.

[4] H. B. Wang, M. H. Wong, C. Y. Lan et al., "Uptake and accumulation of arsenic by 11 *Pteris* taxa from southern China," *Environmental Pollution*, vol. 145, no. 1, pp. 225–233, 2007.

[5] X. Wang, Y. O. Liu, G. M. Zeng et al., "Subcellular distribution and chemical forms of cadmium in *Bechmeria nivea* (L.) Gaud," *Environmental & Experimental Botany*, vol. 62, no. 3, pp. 389–395, 2008.

[6] M. Lei, Q.-L. Yue, T.-B. Chen et al., "Heavy metal concentrations in soils and plants around Shizuyuan mining area of Hunan Province," *Acta Ecologica Sinica*, vol. 25, no. 5, pp. 1146–1151, 2005 (Chinese).

[7] J. Dai, Y. Jie, J. Leng, and Z. Sun, "Distribution of cadmium in different parts of ramie in a polluted environment," *Plant Fiber Production*, vol. 25, pp. 279–293, 2003 (Chinese).

[8] W. She, Y. Jie, H. Xing et al., "Uptake and accumulation of heavy metal by ramie (*Boehmeria nivea*) growing on antimony mining area in Lengshuijiang City of Hunan Province," *Journal of Agro-Environment Science*, vol. 29, no. 1, pp. 91–96, 2010 (Chinese, with English abstract).

[9] Y. Zheng and J. D. Ayotte, "At the crossroads: hazard assessment and reduction of health risks from arsenic in private well waters of the northeastern United States and Atlantic Canada," *Science of the Total Environment*, vol. 505, pp. 1237–1247, 2015.

[10] R. Singh, S. Singh, P. Parihar, V. P. Singh, and S. M. Prasad, "Arsenic contamination, consequences and remediation techniques: a review," *Ecotoxicology and Environmental Safety*, vol. 112, pp. 247–270, 2015.

[11] H. Guo, D. Wen, Z. Liu, Y. Jia, and Q. Guo, "A review of high arsenic groundwater in Mainland and Taiwan, China: distribution, characteristics and geochemical processes," *Applied Geochemistry*, vol. 41, pp. 196–217, 2014.

[12] Z. E.-C. Huang, T.-B. Chen, M. Lei, Y.-R. Liu, and T.-D. Hu, "Difference of toxicity and accumulation of methylated and inorganic arsenic in arsenic-hyperaccumulating and -hypertolerant plants," *Environmental Science and Technology*, vol. 42, no. 14, pp. 5106–5111, 2008.

[13] S. Ismail, F. Khan, and M. Z. Iqbal, "Phytoremediation: assessing tolerance of tree species against heavy metal (Pb and Cd) toxicity," *Pakistan Journal of Botany*, vol. 45, no. 6, pp. 2181–2186, 2013.

[14] D. T. Arnon, "Copper enzyme in isolated chloroplasts polyphenoloxidase in *Beta vulgaris*," *Plant Physiology*, vol. 24, no. 1, pp. 1–15, 1949.

[15] C. J. Huang, G. Wei, Y. C. Jie et al., "Responses of gas exchange, chlorophyll synthesis and ROS-scavenging systems to salinity stress in two ramie (*Boehmeria nivea* L.) cultivars," *Photosynthetica*, vol. 53, no. 3, pp. 455–463, 2015.

[16] S. Ehsan, S. Ali, S. Noureen et al., "Citric acid assisted phytoremediation of cadmium by *Brassica napus* L.," *Ecotoxicology and Environmental Safety*, vol. 106, pp. 164–172, 2014.

[17] H. Metzner, H. Rau, and H. Senger, "Untersuchungen zur Synchronisierbarkeit einzelner pigmentmangel-mutanten von *Chlorella*," *Planta*, vol. 65, no. 2, pp. 186–194, 1965.

[18] R. W. Feng and C. Y. Wei, "Antioxidative mechanisms on selenium accumulation in *Pteris vittata* L., a potential selenium phytoremediation plant," *Plant, Soil and Environment*, vol. 58, no. 3, pp. 105–110, 2012.

[19] R. Feng, C. Wei, S. Tu, F. Wu, and L. Yang, "Antimony accumulation and antioxidative responses in four fern plants," *Plant and Soil*, vol. 317, no. 2, pp. 93–101, 2009.

[20] I. E. Zaheer, S. Ali, M. Rizwan et al., "Citric acid assisted phytoremediation of copper by *Brassica napus* L," *Ecotoxicology and Environmental Safety*, vol. 120, pp. 310–317, 2015.

[21] M. L. Dionisio-Sese and S. Tobita, "Antioxidant responses of rice seedlings to salinity stress," *Plant Science*, vol. 135, no. 1, pp. 1–9, 1998.

[22] S. Jana and M. A. Choudhuri, "Glycolate metabolism of three submersed aquatic angiosperms during ageing," *Aquatic Botany*, vol. 12, no. C, pp. 345–354, 1982.

[23] M. B. Shakoor, S. Ali, A. Hameed et al., "Citric acid improves lead (Pb) phytoextraction in *Brassica napus* L. by mitigating Pb-induced morphological and biochemical damages," *Ecotoxicology and Environmental Safety*, vol. 109, pp. 38–47, 2014.

[24] S. Yamasaki and L. C. Dillenburg, "Measurements of leaf relative water content in *Araucaria angustifolia*," *Sociedade Brasileira de Fisiologia Vegetal*, vol. 11, no. 2, pp. 69–75, 1999.

[25] G. Okkenhaug, Y.-G. Zhu, J. He, X. Li, L. Luo, and J. Mulder, "Antimony (Sb) and Arsenic (As) in Sb mining impacted paddy soil from Xikuangshan, China: differences in mechanisms controlling soil sequestration and uptake in Rice," *Environmental Science and Technology*, vol. 46, no. 6, pp. 3155–3162, 2012.

[26] W. She, Y.-C. Jie, H.-C. Xing et al., "Absorption and accumulation of cadmium by ramie (*Boehmeria nivea*) cultivars: a field study," *Acta Agriculturae Scandinavica Section B: Soil & Plant Science*, vol. 61, no. 7, pp. 641–647, 2011.

[27] W. She, Y.-C. Jie, H.-C. Xing et al., "Tolerance to cadmium in ramie (*Boehmeria nivea*) genotypes and its evaluation indicators," *Acta Agronomica Sinica*, vol. 37, no. 2, pp. 348–354, 2011.

[28] N. Singh, L. Q. Ma, M. Srivastava, and B. Rathinasabapathi, "Metabolic adaptations to arsenic-induced oxidative stress in *Pteris vittata* L and *Pteris ensiformis* L," *Plant Science*, vol. 170, no. 2, pp. 274–282, 2006.

[29] R. Feng, C. Wei, S. Tu, Y. Ding, R. Wang, and J. Guo, "The uptake and detoxification of antimony by plants: a review," *Environmental and Experimental Botany*, vol. 96, pp. 28–34, 2013.

[30] I. Saidi, M. Ayouni, A. Dhieb, Y. Chtourou, W. Chaïbi, and W. Djebali, "Oxidative damages induced by short-term exposure to cadmium in bean plants: protective role of salicylic acid," *South African Journal of Botany*, vol. 85, pp. 32–38, 2013.

[31] C. Huang, G. Wei, Y. Jie et al., "Effects of concentrations of sodium chloride on photosynthesis, antioxidative enzymes, growth and fiber yield of hybrid ramie," *Plant Physiology and Biochemistry*, vol. 76, pp. 86–93, 2014.

[32] S. Silva, G. Pinto, B. Correia, O. Pinto-Carnide, and C. Santos, "Rye oxidative stress under long term Al exposure," *Journal of Plant Physiology*, vol. 170, no. 10, pp. 879–889, 2013.

[33] V. Otones, E. Álvarez-Ayuso, A. García-Sánchez, I. S. Regina, and A. Murciego, "Mobility and phytoavailability of arsenic in an abandoned mining area," *Geoderma*, vol. 166, no. 1, pp. 153–161, 2011.

[34] N. Karimi, S. M. Ghaderian, and H. Schat, "Arsenic in soil and vegetation of a contaminated area," *International Journal of Environmental Science and Technology*, vol. 10, no. 4, pp. 743–752, 2013.

[35] N. Mirza, Q. Mahmood, A. Pervez et al., "Phytoremediation potential of *Arundo donax* in arsenic-contaminated synthetic wastewater," *Bioresource Technology*, vol. 101, no. 15, pp. 5815–5819, 2010.

[36] N. Karimi, S. M. Ghaderian, H. Maroofi, and H. Schat, "Analysis of arsenic in soil and vegetation of a contaminated area in Zarshuran, Iran," *International Journal of Phytoremediation*, vol. 12, no. 2, pp. 159–173, 2010.

Hindawi Publishing Corporation
BioMed Research International
Volume 2016, Article ID 9384767, 7 pages
http://dx.doi.org/10.1155/2016/9384767

Research Article

Synergy between *Rhizobium phaseoli* and *Acidithiobacillus ferrooxidans* in the Bioleaching Process of Copper

Xuecheng Zheng[1,2,3] and Dongwei Li[3]

[1]*College of Chemistry and Chemical Engineering, Southwest Petroleum University, Chengdu 610500, China*
[2]*Oil and Gas Field Applied Chemistry Key Laboratory of Sichuan Province, Chengdu 610500, China*
[3]*College of Resource and Environment Science, Chongqing University, Chongqing 400044, China*

Correspondence should be addressed to Dongwei Li; litonwei@cqu.edu.cn

Received 14 September 2015; Revised 4 December 2015; Accepted 10 January 2016

Academic Editor: Weiqi Fu

This study investigates the synergy of *Rhizobium phaseoli* and *Acidithiobacillus ferrooxidans* in the bioleaching process of copper. The results showed that additional *R. phaseoli* could increase leaching rate and cell number of *A. ferrooxidans*. When the initial cell number ratio between *A. ferrooxidans* and *R. phaseoli* was 2 : 1, *A. ferrooxidans* attained the highest final cell number of approximately 2×10^8 cells/mL and the highest copper leaching rate of 29%, which is 7% higher than that in the group with *A. ferrooxidans* only. *R. phaseoli* may use metabolized polysaccharides from *A. ferrooxidans*, and organic acids could chelate or precipitate harmful heavy metals to reduce their damage on *A. ferrooxidans* and promote its growth. Organic acids could also damage the mineral lattice to increase the leaching effect.

1. Introduction

The environment and natural resources are important topics for research. Many researchers have reported the harmful effects of heavy metals from tailings reservoir on the environment [1, 2]. However, some heavy metals with high value, such as copper, could be recycled from the tailings. Bioleaching is commonly performed on low-grade copper because it is cheaper, more environment friendly, and more efficient than traditional methods [3, 4].

Bacteria require a strict reaction environment during the leaching process; thus, the low leaching rate and inefficiency have become a challenge [5]. Scholars have conducted studied electric fields [6], catalysts [7], metal cations [8], and other related topics to improve the leaching process. The use of synergy among different bacteria is an important approach in improving bioleaching. Donati et al. investigated the collaborative leaching of *Acidithiobacillus ferrooxidans* and *Acidithiobacillus thiooxidans* [9]. Deng et al. discussed the collaborative leaching of *Leptospirillum ferrooxidans* and *A. thiooxidans* [10, 11]. These studies found that mixed cultures demonstrate better performance than pure cultures. Zhu and Zhang found that the synergistic effects between chemoautotrophic bacteria and heterotrophic bacteria can improve the leaching rate of heavy metals [12]. During the leaching process, some additional bacteria could not endure the high concentration of heavy metals or the strong acidic condition. Few researchers have studied the assistance of high-tolerance chemoheterotrophic bacteria in the bioleaching process which could adapt to the environment at pH = 2. Thus, this study selected *Rhizobium phaseoli* to improve the leaching efficiency by using the synergy between *R. phaseoli* and *A. ferrooxidans*. *R. phaseoli* isolated from the nodules of kidney beans (a type of overaccumulated plant) could grow under strict conditions.

2. Materials and Methods

2.1. Materials

2.1.1. Sample. The tailing sample was collected from a copper mine reservoir in Yunnan province, China. Early sample analysis showed chalcopyrite as the main component, with 0.31% copper quality. However, the contents of other heavy

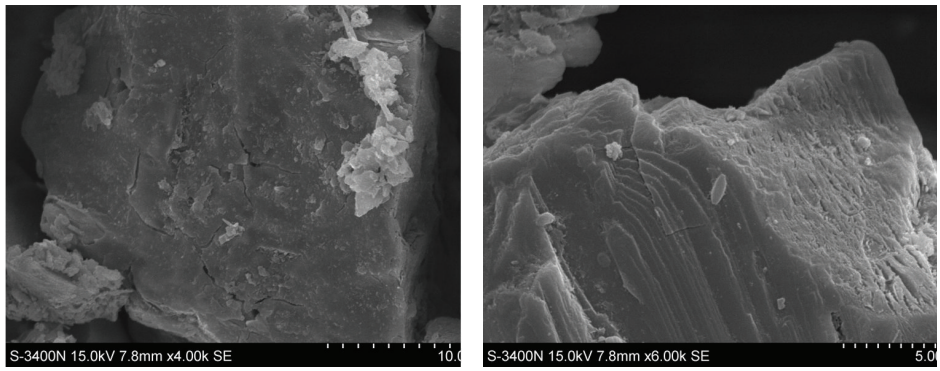

Figure 1: SEM pictures of tailing sample ((4000x) and (6000x)).

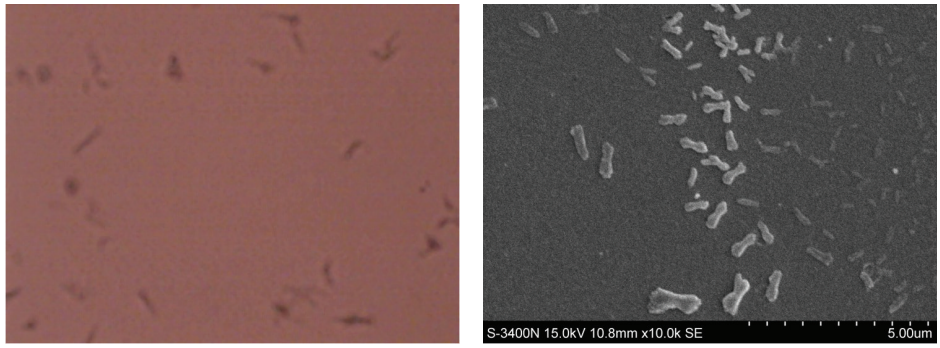

Figure 2: Pictures of *Acidithiobacillus ferrooxidans* under optical microscope (1000x) and SEM (10000x).

metals especially toxic heavy metals (Cd 0.06403 mg/g, Pb 0.33251 mg/g, Ni 0.06227 mg/g, etc.) were too little to affect the bacteria, the average particle size of this sample was 18.30 μm, and the content of sulfur was relatively high to provide the energy for *A. ferrooxidans*, so this tailing sample was suitable for bioleaching. The results of SEM testing and total content of heavy metals are listed in Figure 1.

2.1.2. A. ferrooxidans. The strain was isolated from an acid mine drainage and stored in the biological lab of Chongqing University, China. At the beginning of the experiment, 9K liquid medium was inoculated with the strain and then placed in constant temperature shaking with suitable environment. Only the bacteria in logarithmic phase were used for this experiment. Figures 2 and 3 show *A. ferrooxidans* under optical microscope and SEM, respectively. The pictures under optical microscope and SEM are listed in Figure 2.

2.1.3. R. phaseoli. The strain, which is a type of heterotrophic and aerobic bacteria, was obtained from Agricultural Culture Collection of China and initially isolated from nodules of kidney bean. The strain could use many types of carbon source and grow in acidic environment. After previous domestication, the strain could grow normally in a copper concentration of 0.5 g/L and pH value of 2. The pictures under optical microscope and SEM are listed in Figure 3.

2.1.4. Medium. The medium of *A. ferrooxidans* and *R. phaseoli* was, respectively, 9K liquid medium (composition: 3 g/L $(NH_4)_2SO_4$, 0.5 g/L K_2HPO_4, 0.5 g/L $MgSO_4 \cdot 7H_2O$, 0.01 g/L $Ca(NO_3)_2$, 0.23 g/L $FeSO_4 \cdot 7H_2O$, 0.1 g/L KCl, and 1 L distilled water) and YMA liquid medium (yeast morphology agar, composition: 10 g/L mannitol, 1 g/L yeast powder, 0.5 g/L K_2HPO_4, 0.2 g/L $MgSO_4 \cdot 7H_2O$, 0.1 g/L $CaHPO_4$, 0.1 g/L NaCl, 4 mL 0.5% boric acid solution, 4 mL 0.5% sodium molybdate solution, 10 mL 0.4% Congo red, and 1 L distilled water).

2.1.5. Experimental Equipment. Atomic fluorescence spectrometer (SK-2002B; Beijing, China), vertical pressure steam sterilizer (YXQ-LS-30S; Shanghai, China), constant temperature shaking (THZ-92A; Shanghai, China), pH-ORP tester (ORP-421; Shanghai, China), microscope (XSP-8C; Shanghai, China), thermostatic incubator (LRH-250-A; Shanghai, China), HPLC (Waters 2695; Shanghai, China), and hemocytometer (XB-R-25; Shanghai, China) were used in this experiment.

2.1.6. Analytical Methods. The concentration of copper was tested with atomic fluorescence spectrometer, and leaching rate was defined as the copper concentration in leaching solution divided by the total copper content in the sample. We, respectively, dissolved 100 mg oxalic acid, 100 mg malic acid, 100 mg formic acid, 100 mg acetic acid, 100 mg succinate, 100 mg lactate, and 100 mg citrate with buffer solution to 50 mL, and then we detected organic acids with HPLC after filtration and ultrasonic degassing. The chromatographic conditions were listed as follows: chromatographic column

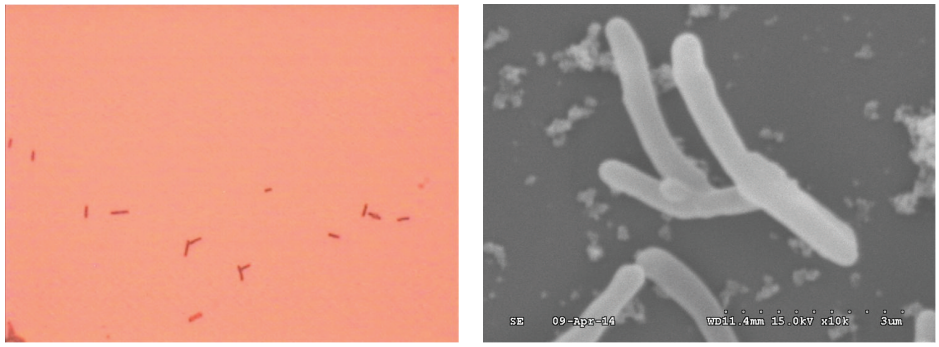

Figure 3: Pictures of *Rhizobium phaseoli* under optical microscope (1000x) and SEM (10000x).

was Hypersil BDS C_{18} (4.6 mm × 250 mm 5 μm), 0.5% $NH_4H_2PO_4$-H_3PO_4 buffer solution was the mobile phase, sample injection volume was 10 μL, temperature was 30°C, flow rate was 1.0 mL/min, and measuring wavelength was 214 nm. We counted the number of bacteria by hemocytometer measurement. At first, we centrifuged or diluted the bacteria liquid until the concentration was at the order of appropriate magnitude and dyed the bacteria with trypan blue; after that we counted the bacteria in the grids for 3 times and calculated the concentration of bacteria with the corresponding formula.

2.2. Experimental Procedure. Tailing sample (10 g) was ground and divided into five groups, with each group containing three parallel test flasks. The first group was the sterile control group, and the other four groups were marked from A to D. *A. ferrooxidans* bacterial liquid (10 mL; 1.1 × 10^7 cells/mL) was added to the four groups A–D. Groups B, C, and D were added with 10, 5, and 1 mL of *R. phaseoli* bacterial liquid (9 × 10^6 cells/mL), respectively. The solution volumes were then adjusted to 100 mL, and noniron 9K liquid medium and initial pH values were adjusted to 2.2 with concentrated sulfuric acid included in all five groups. The initial *A. ferrooxidans*/*R. phaseoli* cell number ratios were about 1 : 1, 2 : 1, and 10 : 1 in groups B, C, and D, respectively, and tailing concentration was 10% (w/v) in each flask. Finally, all the five groups were placed in an air bath oscillator at 100 rpm and 25°C. The experiment lasted for 25 days, the pH values and cell numbers were measured daily, and copper concentrations were measured every 3 days. We calculated the mean values as the final testing results after omitting the finding with obvious errors.

3. Results and Discussion

3.1. Change of pH Values. Figure 4 shows the changes in pH values among the five groups. The pH values in all the groups increased during the first 15 days. This increase was attributed to the reaction of some alkaline substances as chalcopyrite and ferrosulphide compounds with acids in the tailing and the proliferation of *A. ferrooxidans*, which also consumed hydrogen ions in the leaching solution, and the rate of neutralization reaction was much more than the rate of bacterial oxidation reaction. Furthermore, Fe^{2+} would be oxidized into

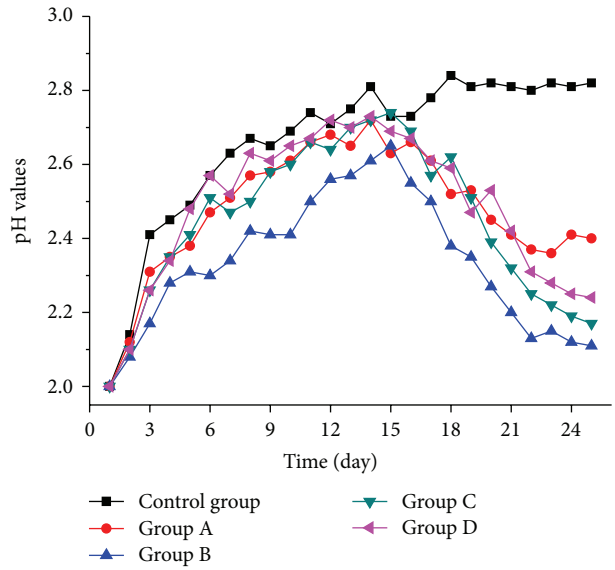

Figure 4: Change of pH values in 5 groups.

Fe^{3+} as the energy of *A. ferrooxidans*; it consumed large number of hydrogen ions as follows:

$$4Fe^{2+} + O_2 + 4H^+ \xrightarrow{\text{bacteria}} 4Fe^{3+} + 2H_2O \quad (1)$$

The pH level in the control group became stable on the 12th day and reached a value of 2.82 by the end of the experiment. The pH levels in the other groups started to decrease from the 16th day because of the near-depletion of alkaline substances and the hydrolysis reaction of Fe^{3+}. With the growth of *A. ferrooxidans*, Fe^{2+} was oxidized to Fe^{3+}, and the hydrolysis reaction of Fe^{3+} continuously advanced and generated numerous hydrogen ions [13]. By the end of the experiment, group B obtained the lowest pH value of 2.11 because more organic acids were secreted by *R. phaseoli* [14].

3.2. Test Results of Organic Acids. Organics, especially those with high content of small molecular organic acids, can cause the cytoplasm acidification of chemoautotrophic bacteria [15]. The reduction of oxygen at the extremity of the electron transport chain could also be affected. Thus, organics can

Table 1: Contents of organic acids in liquid culture mediums (mg/L).

Group	Oxalic acid	Malic acid	Formic acid	Acetic acid	Succinate	Lactate	Citrate
B	78.4	27.3	2.1	13.7	8.6	Not detected	36.9
C	74.2	31.1	1.7	10.9	7.9	Not detected	34.1
D	69.1	24.9	2.3	11.2	1.8	Not detected	31.8

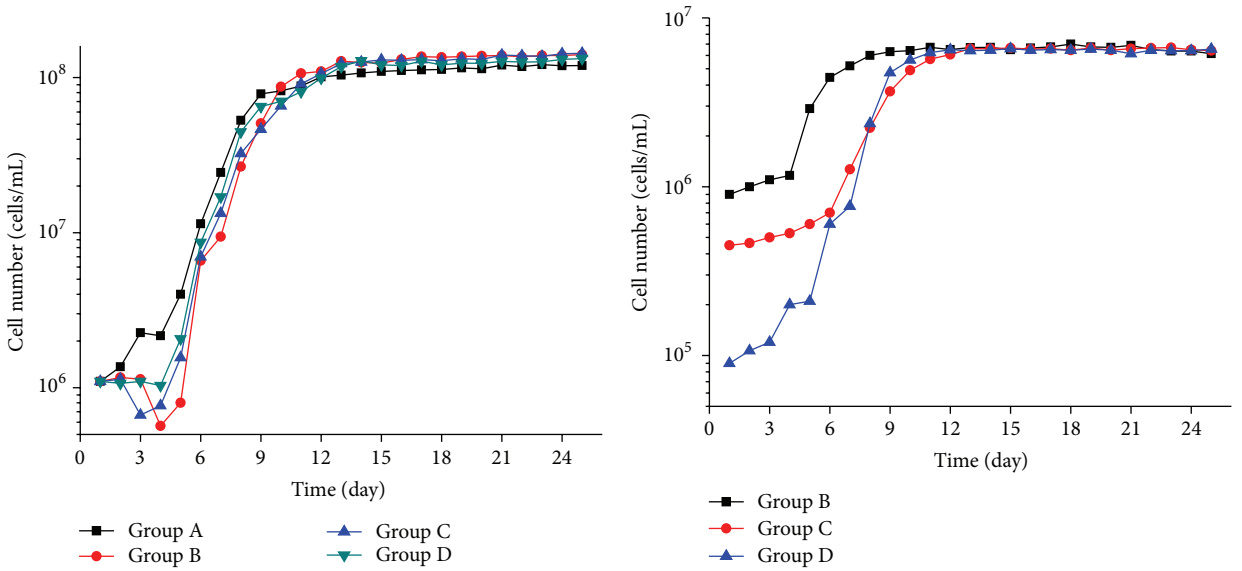

(a) The cell number of *A. ferrooxidans*

(b) The cell number of *R. phaseoli*

Figure 5: The cell number (ordinate after logarithmic transformation) of *Acidithiobacillus ferrooxidans* (a) and *Rhizobium phaseoli* (b).

damage the growth and metabolism of *A. ferrooxidans*. Organic acids were the main metabolites of *R. phaseoli*. We measured the contents of small molecular organic acids in groups B, C, and D with HPLC. The results are listed in Table 1.

As shown in Table 1, oxalic acid was the organic acid with the highest concentration (78.4 mg/L), whereas lactate was undetected. The concentration of formic acid, which is the most harmful acid to *A. ferrooxidans*, was relatively low [16]. Some studies showed that *A. ferrooxidans* can grow normally when the content of acetic acid or oxalic acid is ≤100 mg/L [17]. However, the proper content of organic acids can even stimulate the metabolic ability of Fe^{2+} in *A. ferrooxidans*.

3.3. Changes of the Cell Number of Bacteria. Figure 5 shows the changes of the cell number of *R. phaseoli* and *A. ferrooxidans*. *R. phaseoli* could also grow normally without an added YMA liquid medium, and the remaining YMA medium in the previous bacteria liquid might provide the carbon source for *R. phaseoli*. However, *R. phaseoli* might have also used *A. ferrooxidans* metabolites as its carbon source. The logarithmic phase in group B with the most initial *R. phaseoli* was the shortest, and the stable phase in group B was also the earliest. In the last few days, the cell number of *R. phaseoli* in all the three groups tended to be stable and similar (about 5×10^6 cells/mL) because the nutrients for *A. ferrooxidans* in the 9K medium added into the leaching environment were limited, and a certain number of *A. ferrooxidans* could provide

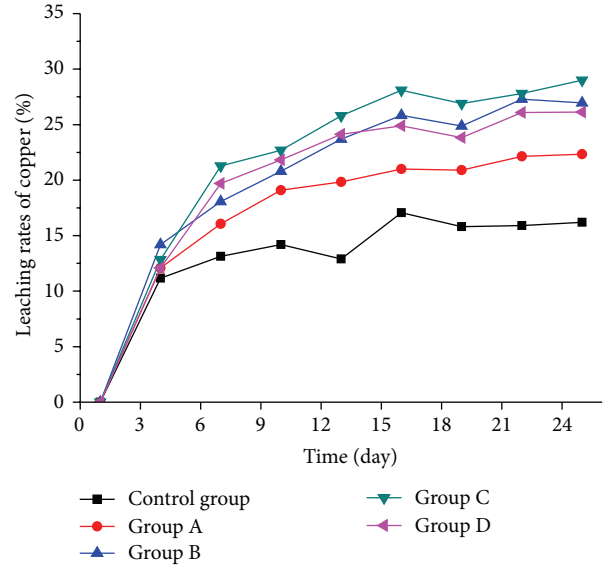

Figure 6: The changes of copper leaching rates.

limited organic compounds for *R. phaseoli*. Therefore, the differences became small toward the end of the experiment.

At the beginning of the experiment, the adaptation period of *A. ferrooxidans* in groups B, C, and D (with *R. phaseoli*) was evidently longer than that in group A (without *R. phaseoli*). This result may be attributed to the higher initial *R. phaseoli*

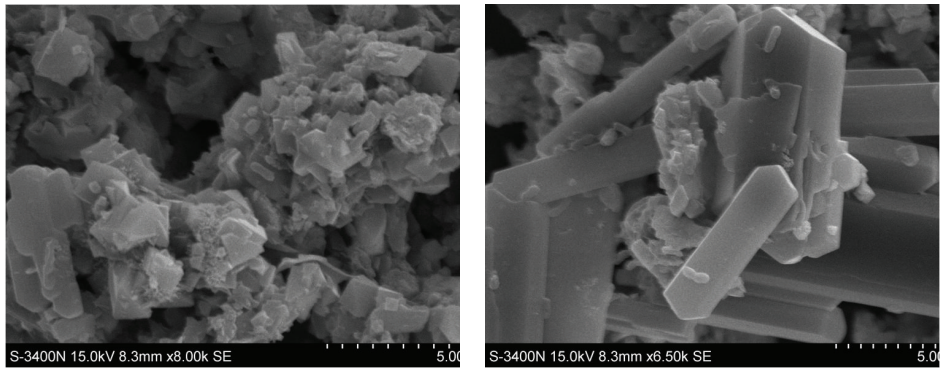

(8000x) (6500x)

Figure 7: SEM pictures of tailing sample after leaching.

concentration, which resulted in a longer adoption phase. The two reasons for this phenomenon are as follows. (1) The metabolites of *R. phaseoli* (mainly organic acids) inhibited the growth of *A. ferrooxidans* to some extent. (2) *R. phaseoli* competed with *A. ferrooxidans* for other sources, such as dissolved oxygen; thus, *A. ferrooxidans* needed more time to adapt to the new environment.

At the end of the experiment, the numbers of *A. ferrooxidans* in groups B, C, and D were, respectively, 1.4×10^8 cells/mL, 1.43×10^8 cells/mL, and 1.33×10^8 cells/mL, which is about 2×10^7 cells/mL more than 1.16×10^8 cells/mL in group A. The main compositions of extracellular polymeric substances (EPS) of *A. ferrooxidans* were glucose, rhamnose, nucleic acid, and protein. *R. phaseoli* are chemoheterotrophic bacteria that consume metabolites in the EPS of *A. ferrooxidans* as complex organics were hydrolyzed into simple organics, ATP, and [H] under the action of catabolism enzyme.

The negative effect of organic acids on *A. ferrooxidans* could be reduced. The low concentration of organic acids could not harm *A. ferrooxidans* but could stimulate its growth. Organic acids released by *R. phaseoli* could chelate or precipitate the harmful heavy metals in the solution and could reduce the hazard to *A. ferrooxidans* [15].

3.4. Changes of the Leaching Rate of Copper. Figure 6 shows the changes in copper leaching rates among the five groups. During the first four days, the differences among the five groups were not evident, and the leaching rates in groups with bacteria were obviously higher than that in the control group from the fourth day. The leaching rates in groups B, C, and D were higher than that in group A from the fourth day, as well. At the end of this experiment, the leaching rate of group A was 22.3%, which is 6.1% higher than that in the control group 16.2%, proving that *A. ferrooxidans* could promote copper leaching. Additional *R. phaseoli* could further raise the leaching rate to 29%, especially in group C, where the initial *A. ferrooxidans*/*R. phaseoli* cell number ratio was 2 : 1. At the 25th day, the leaching rates in groups B and D were 27% and 26.1%, respectively. The leaching results provided evidence that adding *R. phaseoli* could promote copper leaching further due to the reasons mentioned previously.

Figure 7 shows the tailing sample with bacteria on its surface in the leaching process. *A. ferrooxidans* adsorbed on the surface with its flagellum at the beginning. The bacteria oxidized minerals and obtained energy with the oxidizing enzymes of Fe^{2+} and S, and then the electrons released in the chemical oxidation reached the plasma membrane which was the combined point of bacterial respiration, *A. ferrooxidans* destroyed the surface lattices of metal sulfide minerals to oxidize them to the metal ions directly as mentioned earlier or oxidized Fe^{2+} into Fe^{3+}, and then Fe^{3+} oxidized minerals with its strong oxidative activity. The direct and indirect mechanisms [18] are shown in Figure 8.

R. phaseoli could improve the growth and activity of *A. ferrooxidans*. Moreover, *R. phaseoli* mainly secreted organic acids, such as oxalic acid and citric acid. Oxalate anions contain strong and stable electrons, and each citric acid molecule can ionize three hydrogen ions. Thus, both oxalic acid and citric acid are strong organic acids that could damage mineral lattices to release copper ions into the leaching solution.

4. Conclusions

This study investigated the synergy between *R. phaseoli* and *A. ferrooxidans* in the bioleaching process. The cell number of *A. ferrooxidans* evidently increased because *R. phaseoli* consumed some of the organic metabolites of *A. ferrooxidans*. The number in group C was the highest at the beginning of the 8th day, and organic acids could chelate or precipitate harmful heavy metals to reduce their negative influence on *A. ferrooxidans*. Therefore, the cell number of *A. ferrooxidans* increased, whereas the cell number of *R. phaseoli* in the three groups tended to be stable and similar. The leaching results showed that *R. phaseoli* could obviously increase the copper leaching rate from 22% to 29%. In addition to the increase in the number of *A. ferrooxidans*, organic acids could also damage the mineral lattices to release copper ions into leaching solution. However, the low concentration of organic acids did not exceed the endurance limit of *A. ferrooxidans* and even promoted the leaching efficiency.

Research Gap and Outlook. This study found that the synergy between *Rhizobium phaseoli* and *Acidithiobacillus*

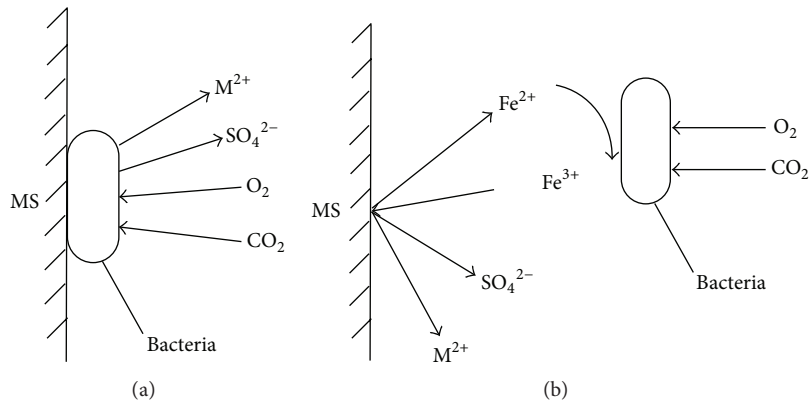

Figure 8: The schematic diagram of direct (a) and indirect leaching mechanism (b).

ferrooxidans could promote copper leaching efficiency, but the leaching rate remained low and took a long time. For future work, the authors aim to investigate the catalyst for accelerating the leaching rates.

Conflict of Interests

The authors declare no conflict of interests.

Authors' Contribution

Dongwei Li conceived and designed the experiments; Xuecheng Zheng performed the experiments and analyzed the data.

Acknowledgment

The work was supported by the Young Scholars Development Fund of SWPU (no. 201499010071).

References

[1] N. Rogan, T. Serafimovski, M. Dolenec, G. Tasev, and T. Dolenec, "Heavy metal contamination of paddy soils and rice (*Oryza sativa* L.) from Kočani Field (Macedonia)," *Environmental Geochemistry and Health*, vol. 31, no. 4, pp. 439–451, 2009.

[2] D. Alexakis, "Human health risk assessment associated with Co, Cr, Mn, Ni and V contents in agricultural soils from a Mediterranean site," *Archives of Agronomy and Soil Science*, vol. 62, no. 3, pp. 359–373, 2015.

[3] S. Y. Chen, L. G. Lin, and C. Y. Lee, "Effects of ferric ion on bioleaching of heavy metals from contaminated sediment," *Water Science and Technology*, vol. 48, no. 8, pp. 151–158, 2003.

[4] H. R. Watling, "Chalcopyrite hydrometallurgy at atmospheric pressure: 2. Review of acidic chloride process options," *Hydrometallurgy*, vol. 146, pp. 96–110, 2014.

[5] K. M. M. Aung and Y.-P. Ting, "Bioleaching of spent fluid catalytic cracking catalyst using *Aspergillus niger*," *Journal of Biotechnology*, vol. 116, no. 2, pp. 159–170, 2005.

[6] H. Zuo, A.-X. Wu, and Y.-M. Wang, "Effect of electric field on improving leaching ability of microbe," *Chinese Journal of Nonferrous Metals*, vol. 17, no. 7, pp. 1177–1181, 2007.

[7] H. Nakazawa, H. Fujisawa, and H. Sato, "Effect of activated carbon on the bioleaching of chalcopyrite concentrate," *International Journal of Mineral Processing*, vol. 55, no. 2, pp. 87–94, 1998.

[8] E. Gómez, A. Ballester, M. L. Blázquez, and F. Gonzáez, "Silver-catalysed bioleaching of a chalcopyrite concentrate with mixed cultures of moderately thermophilic microorganisms," *Hydrometallurgy*, vol. 51, no. 1, pp. 37–46, 1999.

[9] E. Donati, G. Curutchet, C. Pogliani, and P. Tedesco, "Bioleaching of covellite using pure and mixed cultures of *Thiobacillus ferrooxidans* and *Thiobacillus thiooxidans*," *Process Biochemistry*, vol. 31, no. 2, pp. 129–134, 1996.

[10] T. L. Deng and M. X. Liao, "Gold recovery from the refractory flotation concentrate combined biooxidation and thiourea leach," *Hydrometallurgy*, vol. 63, no. 3, pp. 249–255, 2005.

[11] L. Falco, C. Pogliani, G. Curutchet, and E. Donati, "A comparison of bioleaching of covellite using pure cultures of *Acidithiobacillus ferrooxidans* and *Acidithiobacillus thiooxidans* or a mixed culture of *Leptospirillum ferrooxidans* and *Acidithiobacillus thiooxidans*," *Hydrometallurgy*, vol. 71, no. 1-2, pp. 31–36, 2003.

[12] J. Y. Zhu and J. X. Zhang, "Bioleaching of heavy metals from contaminated alkaline sediment by auto and heterotrophic bacteria in stirred tank reactor," *Transactions of Nonferrous Metals Society of China*, vol. 24, no. 9, pp. 2969–2975, 2014.

[13] S. Bhattacharyya, B. K. Chakrabarty, A. Das, P. N. Kundu, and P. C. Banerjee, "*Acidiphilium symbioticum* sp.nov., an acidophilic heterotrophic bacterium from *Thiobacillus ferrooxidans* cultures isolated from Indian mines," *Canadian Journal of Microbiology*, vol. 37, no. 1, pp. 78–85, 1991.

[14] L. Zhang and J. G. Huang, "Mobilization of potassium from soils by *Rhizobium phaseoli*," *Acta Ecologica Sinica*, vol. 32, no. 5, pp. 996–1002, 2012.

[15] B. Alexander, S. Leach, and W. J. Ingledew, "The relationship between chemiosmotic parameters and sensitivity to anions and organic acids in the acidophile *Thiobacillus ferrooxidans*," *Journal of General Microbiology*, vol. 133, no. 5, pp. 1171–1179, 1987.

[16] H. W. Liu and Y. X. Dai, "Effects of low molecular weight organic acids on *Acidithiobacillus ferrooxidans*," *Journal of Environmental Engineering*, vol. 9, pp. 1269–1272, 2003.

[17] W. X. Ren and P. J. Li, "Effects of low molecular weight organic acids on *Acidithiobacillus ferrooxidans*," *Chinese Journal of Environmental Engineering*, vol. 2, no. 9, pp. 1260–1273, 2009.

[18] H. Tributsch, "Direct versus indirect bioleaching," *Hydrometallurgy*, vol. 59, no. 2-3, pp. 177–185, 2001.

Hindawi Publishing Corporation
BioMed Research International
Volume 2016, Article ID 1397852, 9 pages
http://dx.doi.org/10.1155/2016/1397852

Research Article

Extraction of Oleic Acid from Moroccan Olive Mill Wastewater

Reda Elkacmi,[1,2] Noureddine Kamil,[2] Mounir Bennajah,[3] and Said Kitane[3]

[1]*Department of Chemistry and Valorisation, Faculty of Sciences Ain-Chock, HASSAN II University of Casablanca, BP 5366 Maarif, Casablanca, Morocco*
[2]*Process Engineering and Environment Laboratory (PEEL), High School of Technology of Casablanca, HASSAN II University of Casablanca, BP 8012 Oasis, Casablanca, Morocco*
[3]*Department of Process Engineering, National School of Mineral Industries of Rabat, BP 753 Agdal, Rabat, Morocco*

Correspondence should be addressed to Reda Elkacmi; redakcm@gmail.com

Received 27 October 2015; Revised 26 November 2015; Accepted 7 December 2015

Academic Editor: Hongbing Liu

The production of olive oil in Morocco has recently grown considerably for its economic and nutritional importance favored by the country's climate. After the extraction of olive oil by pressing or centrifuging, the obtained liquid contains oil and vegetation water which is subsequently separated by decanting or centrifugation. Despite its treatment throughout the extraction process, this olive mill wastewater, OMW, still contains a very important oily residue, always regarded as a rejection. The separated oil from OMW can not be intended for food because of its high acidity of 3.397% which exceeds the international standard for human consumption defined by the standard of the Codex Alimentarius, proving its poor quality. This work gives value addition to what would normally be regarded as waste by the extraction of oleic acid as a high value product, using the technique of inclusion with urea for the elimination of saturated and unsaturated fatty acids through four successive crystallizations at 4°C and 20°C to have a final phase with oleic acid purity of 95.49%, as a biodegradable soap and a high quality glycerin will be produced by the reaction of saponification and transesterification.

1. Introduction

The production of Moroccan olive oil has been growing and its consumption has also increased (3.9 kg/inhabitant) in 2013 [1], thanks to its nutritional, medical, and economic importance; it participates with 5% in the Moroccan agricultural GDP and 15% in agrifood exports [2]. Morocco is one of the Mediterranean countries concerned with the attractive developing production of olive oil, with an annual production capacity of 1.5 million tons of olives (amount of 0.6 million tons is triturated by about 565 modern units and semimodern ones and amount of 0.16 million tons of olives per year is triturated by 15,000 traditional units called maâsra) [3]. Alongside their activities, these traditional factories produce solid waste called pomace, mainly used in composting [4], combustible [5], biogas [6], tanning [7], or animal feed [8], and also liquid waste called "Olive Oil Mill Wastewater (OMW)," a variation amount between 0.5 and 1.5 m^3 per 1 ton of olives according to the production method [9]. The "vegetation water" is sent directly to the environmental medium which poses a serious environmental problem because it contains in addition to the acidic pH significant quantities of organic matter and poorly biodegradable polyphenols.

The composition of this olive mill wastewater varies depending on several factors such as the variety and maturity of the olives, the period of production, the climatic conditions, farming methods, and the oil extraction mode [10]. The main physicochemical characteristics of the olive mill wastewater of the region of Fes Boulemane [11] are given in Table 1.

The physicochemical characterization of OMW of the region of Fes Boulemane shows that this effluent has an acid pH value, with a very high chemical oxygen demand (COD) which proves that the OMW constitutes an important environmental problem.

Many biotechnological applications have been made to utilize these liquids that we mentioned; the most commonly used application shown is as follows.

(1) The Lagooning. This natural purification process reduces the load rejection in organic matter and polyphenols existing

Table 1: The main physicochemical characteristics of Moroccan olive mill wastewater.

Parameters	Values
pH	4.7
Acidity (%)	1.3
FM (%)	1
SM (g/L)	0.5
EC (mS/cm)	18.7
COD (g O_2/L)	84.1
BOD_5 (g O_2/L)	30
PP (g/L)	0.2
TNK (g N/L)	0.1
Chlorides (g/L)	5.1

FM: fat matter, SM: suspended matter, EC: electrical conductivity, COD: chemical oxygen demand, BOD_5: biochemical oxygen demand, PP: polyphenols, and TNK: total nitrogen Kjeldahl.

in the olive mill wastewater, to obtain treated water that meets the physicochemical quality standard; it is based on the collection of OMW in ponds outdoors. The organic matter is degraded under the effect of the biological activity of microorganisms, leading to water denitrification [12–15].

This method has the disadvantages of excessive area requirement, the release of bad odors, and the infiltration of pollutants in the basement to land groundwater.

(2) The Composting. Composting of OMW is a technique used to improve the physical, chemical, and biological properties of soil. It is based on the decomposition of organic matter into stable products rich in humic compounds.

Several studies on composting of OMW were conducted [16–18]. This technique improves the water retention in sandy soils and aggregate stability and the cation exchange capacity, which increases microbial activity, and promotes the degradation of pesticides and other organic compounds [19].

(3) Use as Fertilizer. Due to environmental restrictions of the lagooning process of OMW, it can be used as a fertilizer. The high organic load and the concentration of soluble nutrients gives it wide use in agriculture [20, 21].

But its high pollution load, toxicity, and transport costs may limit the use of OMW as fertilizers.

(4) Use as Animal Feed. The high content of sodium and phenolic compounds in the OMW causes digestive disorders in ruminants [22]. Concerning this problem, research has therefore focused on reducing phenols by specific processes. Dalmolive process [23, 24] reduces phenol to an acceptable tenor. 29 kg of food can be produced by combining 50 kg of OMW with 20 kg of exhausted pomace and 12.6 kg of agricultural derivatives.

(5) Biogas Production. The anaerobic digestion process is based on the biochemical conversion of organic matter to produce carbon dioxide and methane [25–27].

A volume of 1 m^3 of OMW contains a concentration of 70 kg of chemical oxygen demand (COD) producing about 24.5 m^3 of methane. The energy of the biogas is used in thermal form and can be converted into electrical energy [28].

Physicochemical and electrochemical processes were used to treat this effluent in order to reduce the organic matter and toxicity to acceptable limits such as lime treatment [29, 30], coagulation-flocculation-hydrogen peroxide oxidation [31], and phenolic treatment [32–34].

The principal aim of the present work was to develop a simple and easy method to recover valuable products from these effluents, discharged directly into the environment with huge amount without effective treatment.

The originality of this work lies in the separation by a natural setting of oil from olive mill wastewater, and after several analyses of this separated oil, we found its acidity higher than human consumption standard, which requires searching recovery solutions by adaptation and application of a fractional extraction technique of fatty acid from these effluents for their valuation coupled on one hand to produce soap and glycerin and on the other hand to extract pure oleic acid contained in this extracted oil.

2. Materials and Methods

After the extraction of olive oil by pressing or centrifuging, the resulting liquid contains oil and vegetation water; the latter is separated by decanting or centrifugation.

Despite their treatment, the rejects from decantation and centrifuging still contain very important oily residues, usually discarded in the environmental media.

The residual oil after separation of OMW may not be used for consumption for its high acidity (it reaches about 3.397%), value exceeding the Codex Alimentarius standard [35].

In our work, we collected 90 L of OMW in the region of Fes Boulemane and after storage in cans of 5 liters, they are preserved in the laboratory for six months at room temperature for decantation.

2.1. Olive Mill Wastewater Characterization. Olive mill wastewater used in this work was collected from diverse traditional crushing units of Fes Boulemane region, during the olive oil year 2012/2013.

The source and mass fraction purity of materials are listed in Table 2.

2.2. Analyses

2.2.1. Oil Analysis. The chemical characterization of recovered oil samples and the soap product was performed according to the method of the International Organization for Standardization (ISO) [36–46].

2.2.2. Samples Analysis by GC. The gas chromatography can be applied directly to fatty acids and fatty esters. Regarding triglycerides, they are used for the study of chain length after conversion into methyl esters.

During separation, samples were analyzed using a gas chromatography having the following characteristics:

Name: VARIANT 304 CX.

Column length: 50 m.

Table 2: Source and mass fraction of material.

Material	Source	Purity % mass
Sodium hydroxide	VWR International	98%
Sodium chloride	VWR International	99.5%
Potassium hydroxide	VWR International	85%
Hydrochloric acid	VWR International	37%
Ethanol	VWR International	95%
Methanol	VWR International	99.9%
Hexane	VWR International	95%
Acetone	VWR International	99%
Iodine monochloride	VWR International	98%
Sodium thiosulfate	VWR International	99.50%
Acetic acid	VWR International	99.90%
Potassium iodide	VWR International	99%
Ethyl oxide	VWR International	≥99.5%
Chloroform	VWR International	≥99%
Starch, soluble	VWR International	99.00%
Phenolphthalein	VWR International	99.00%
Urea	VWR International	≥99%
Anhydrous sodium sulfate	VWR International	99.00%

Stationary phase: silica.

Carrier gas: He.

T column: 210°C.

Detector: FID (Flame Ionization Detector).

2.2.3. Determining Density. For measuring the density, our sample is weighed with a balance and then placed into a graduated cylinder filled with 100 mL of water.

The elevation value of water volume in the graduated cylinder has allowed us to calculate the value of the density.

2.2.4. Determining Boiling Point. To characterize our resultant products we determined their boiling point, by placing the samples (oleic acid, glycerol) in a test tube and a thermometer in place, after heating with a hotplate until the appearance of the first bubble of vapor, the boiling temperature was determined by the thermometer at atmospheric pressure.

2.2.5. Determining Melting Point. The Thiele tube is used to determine the melting point of our products, the sample is placed in a capillary connected with a thermometer and immersed in the tube, and after heating the product began to melt where we note the melting temperature.

2.3. Extraction of Oleic Acid. Oleic acid ((9Z)-octadec-9-enoic acid) is an unsaturated fatty acid. This essential compound of chemistry is also used as a surfactant to modify the surface of magnetite particles [47], in the pharmaceutical field [48], and is considered as a raw material for the production of bioproducts little available in nature [49].

Several techniques have been developed to extract the oleic acid from food waste; the most frequently used one is based on the fractional distillation [50, 51] and the method of inclusion with urea [52, 53]; it remains more advantageous not only because of its lower cost and its better yield, but also because of the quality of the recovered acid, as well as the low temperature adopted for the extraction protecting oleic acid oxidation.

In this work, the method based on the fractional crystallization of urea described by Frémont and Gozzelino [54] was adopted. It thus permits the recovery of a highly purified oleic acid with a very good quality; the difference was that they worked with olive oil; then we can recover this acid by OMW.

2.3.1. Transesterification. The aim of this technique is to transform the triglycerides which constitute the oil, to methyl esters. For this purpose, 200 mL of this oil sample was mixed with 600 mL of methanol. The reaction is catalyzed by 100 mL of sodium methoxide (prepared before by mixing of 1 g of sodium hydroxide with 100 mL of methanol). The mixture is subjected to heating under reflux for 3 hours at 60°C period considered sufficient for a perfect homogenization of the mixture.

The mixture is then separated in a separatory funnel for 4 hours until the appearance of two phases: a top layer rich in methyl ester and a lower layer rich in glycerol. After the recovery of the latter, the separated upper phase is washed properly with hydrochloric acid to neutralize excess sodium hydroxide.

This upper phase of the first separation is rewashed a second time with 100 mL of distilled water, and to form two layers, the upper one rich in pure methyl esters and the lower one rich in water and methanol.

After separating the esters from the upper phase, the lower phase is thus introduced into a separatory funnel in the presence of hexane. A three-stage separation is performed to maximize recovery of methyl esters, successive additions of hexane were made at a rate of 25 mL, and each addition is followed by a separation by decantation. After the adding of the pure methyl esters recovered in the first separation to that extracted by hexane, the mixture was concentrated in the rotatory evaporator, and the esters thus purified were also weighed with an electronic scale.

2.3.2. Crystallization with Urea. The objective of this step is to crystallize methyl oleate by the four successive crystallizations with a purity of about 95. 5% from the methyl esters of fatty acids prepared.

For a first separation, we take 100 g of methyl esters mixed with 100 g of urea and 1 L methanol, using a water bath to achieve solubilization in alcohol.

After cooling overnight at 4°C, our solution is filtered on sintered glass, under vacuum of 1 bar maintained with a vacuum pump (KNF NEUBERGER), trying to keep the same conditions to obtain two phases solid C1 and filtrate F1.

The filtrate F1 is mixed with 200 g of urea. The mixture was maintained at 4°C, to have C2 crystals that will be rinsed and mixed with 1.5 L of methanol and filtered under the vacuum at room temperature.

Filtrate F3 product of the second crystallization is subjected to a temperature of 4°C after adding 120 g of urea.

Table 3: Characteristics of recovered oil from OMW.

Parameters	Values	Norm Codex	Methods
Acidity (%)	3.397	0.3–1	ISO 660 (determination of acid value and acidity)
Iodine index (g/100 g)	82.17	75–94	ISO 3961 (determination of iodine value)
Peroxide index (meq O_2/kg)	11.26	≤20–≤15	ISO 3960 (determination of peroxide value)
Saponification index (mg KOH/g)	189	184–196	ISO 3657 (determination of saponification value)
Refractive index (n_{20}^d)	1.4678	1.4677–1.4705	ISO 6320 (determination of refractive index)

The mixture is allowed to rest until the appearance of crystalline phase C4.

This final phase additionally contains methyl esters urea which must be removed by a hydrochloric acid solution and separated after a natural decantation. These esters are then extracted with hexane, and the excess of acid was removed by pure water and then dried over anhydrous sodium sulfate.

After the removal of the solvent with the rotary evaporator, we weighed resulting esters.

2.4. Saponification. For soap from OMW fast saponification is performed, using a strong base in reflux mounting [55].

2.4.1. Implementation of the Saponification Reaction. A volume of 150 mL of oil recovered from OMW is mixed with 150 mL of ethanol in the presence of 30% sodium hydroxide as an alkaline agent without forgetting a few grains of pumice.

The mixture was kept heating under reflux for 4 hours at 50°C, period deemed sufficient enough for the completion of the saponification reaction until the solution becomes limpid, and our mixture is allowed to settle for a few minutes. The reaction mixture is then separated into two phases, an aqueous one rich in glycerin and a second heavier one which is soap.

The reaction mixture was treated with a solution containing 200 g/L of sodium chloride; the neutralization of NaOH significantly improves the separation of the two phases.

2.4.2. Separation by Filtration. The reaction mixture undergoes a night of natural decantation, for 12 hours. Then, it was vacuum filtered by suction on Büchner funnel through a filter cloth (40 μm). The recovered solid phase (soap) was washed two times with 50 mL of distilled water and dried by sunshine.

2.5. Extraction of Glycerin. Glycerol (propane-1,2,3-triol) is a coproduct which has three hydroxyl groups, functionalisable and used in food [56, 57] and cosmetics [58, 59]; there are two types of glycerol, a synthetic one obtained by the petrochemical process in which propene is converted to glycerol and natural one formed in the two processes of saponification and transesterification [60].

After separation of the aqueous alkaline phase, we will neutralize it with concentrated hydrochloric acid at 12%. After a simple distillation followed by evaporation we can isolate the glycerin (or glycerol).

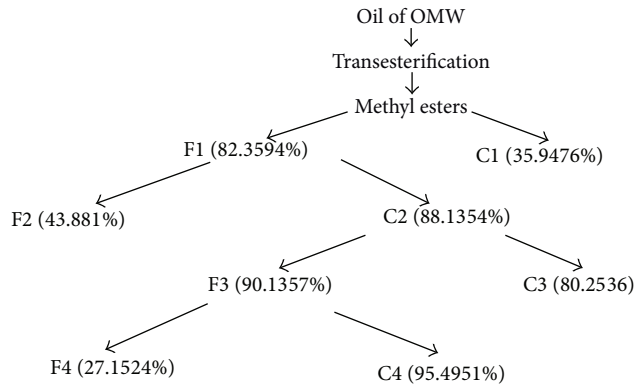

Figure 1: Fractional crystallization steps.

3. Results and Discussion

The oil of OMW was recovered by natural decantation for six months; the 90 liters gave 20 liters (yield 23%). This value is slightly higher proving that despite these effluents treatment remains rich in oil. The characteristics of this oil are shown in Table 3.

Examination of the recovered oil characteristics has shown that the acidity is greater than that for the Codex Alimentarius standard due to lack of oil stability, bad storage conditions, and low peroxide index explained by resistance to oxidation during storage.

After a series of fractional crystallizations, we could have in the end crystallized phase C4 rich in methyl oleate with a purity of 95.49% (Figure 1).

We find that during these four successive separations most of oleic acid either in the crystal or in the filtrate depends on the temperature conditions and dilution.

The majority of saturated fatty acids are eliminated in the first separation at a temperature of 4°C, in the same condition and by adding the urea to the filtrate F1; the rest will be eliminated in the second crystallization, which gives rise to phase C2 having in addition to the oleic acid an amount of saturated fatty acid.

This phase will be diluted with methanol at 20°C to prevent the formation of inclusions, with the elimination of fatty acids, and recover oleic acid in filtrate F3 with 90.1357% purity.

Table 4: Evolution of compounds during separation (% mass fraction).

Fatty acids	Structure	Composition	F1	C1	F2	C2	F3	C3	F4	C4
Palmitic acid	C16:0	9.3429	2.1019	38.8984	0.2920	4.2546	1.7856	12.9456	1.0024	2.5164
Palmitoleic acid	C16:1	0.6096	1.6539	0.0357	2.8123	2.2454	2.5475	4.5789	6.6221	1.9015
Stearic acid	C18:0	2.9059	0.0476	13.9547	0.2225	0.1614	—	—	—	—
Oleic acid	C18:1	74.018	82.3594	35.9476	43.881	88.1354	90.1357	80.2536	27.1524	95.495
Linoleic acid	C18:2	10.9884	12.2856	4.8458	46.5568	3.6213	5.4456	2.2219	64.6214	1.5654
Linolenic acid	C18:3	2.1352	1.5516	6.3178	6.2354	1.5819	0.0856	—	0.6017	0.4231

Table 5: Characteristics of separated oleic acid.

Parameters	Literature [54]	Values
Density	—	0.898
Boiling point (°C)	—	360
Melting point (°C)	14< <15	13.7

A final crystallization gave us by the addition of urea at 4°C a final phase rich in oleic acid (95.4951%).

The evolution in the composition of fatty acids in the four crystallizations is mentioned in Table 4.

In the first separation we could eliminate the saturated acids C16:0 (palmitic acid) and C18:0 (stearic acid) with significant fractions 38.8984% and 13.9547%, respectively. After the second crystallization we could recover in filtrate F2 some of these saturated acids and a part of the unsaturated acids including oleic acid.

C2 crystals contain a small amount of saturated acids which will be crystallized in the third separation where we have used a large amount of methanol at room temperature to form inclusions with these acids. We have also seen a significant distribution of our oleic acid in both phases C3 (80.2536%) and F3 (90.1357%).

In the fourth crystallizing filtrate F3 gave birth to crystalline phase C4 with a highly pure oleic acid and (2.5164%) of palmitic acid and traces of other unsaturated acids.

We can separate oleic acid, using saponification followed by addition of hydrochloric acid, until the occurrence of an oleic acid precipitate whose characteristics are presented in Table 5.

The resulting oleic acid has a yellow color; it is insoluble in water and soluble in some solvent such as ethanol, ether, and chloroform; this product is used to prepare esters, alcohols, and organometallic salt.

With the quality and purity of this compound, we can produce biodiesel by esterification with alcohol.

The oxidative cleavage of the acid produces two unsaturated carboxylic acids: azelaic acid (or acid nonanedioic) used in the cosmetic and pharmaceutical field (treatment of skin diseases including acne) and pelargonic acid (or nonanoic acid) frequently used as fragrance for perfumes, antibacterial, surfactants, and others [61, 62]. Figure 2 shows the variation

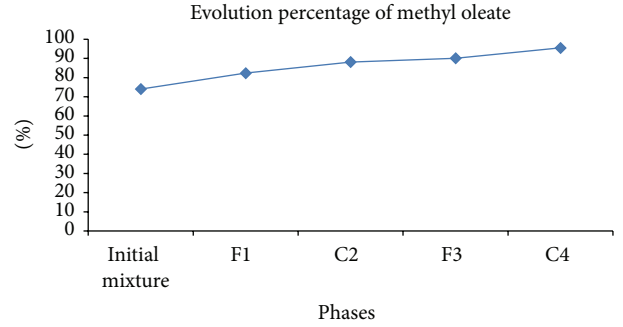

Figure 2: Composition of methyl oleate in phases during crystallization.

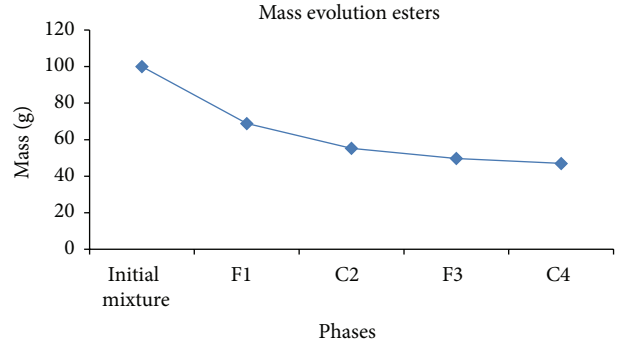

Figure 3: Evolution esters mass during crystallization.

of the composition of methyl oleate during the stages of crystallization.

The initial mixture (separated oil) contains 74.018% methyl oleate, and after the first crystallization we are left with a percentage of 82.3594%; C2 crystals resulting from the second separation have a purity of 88.1354%. F3 and C4 contain 90.1357% and 95.495%, respectively. Frémont et al. were able to extract an oleic acid with purity of 99.5% but by starting from an olive oil and cooling to −60°C of final phase C4 mixed with an acetone solution.

The purity of our oleic acid is of the order of 95.4951%, which is acceptable because we are working with olive mill wastewater instead of virgin olive oil.

Transesterification of 200 mL oil gave approximately 180.65 g of methyl esters where 100 g is used for crystallization. After separating the four were able to get final phase C4 with mass of 46.98 g (Figure 3).

Table 6: Characteristics of the resulting soap.

Parameters	Values	Literature [63]	Methods
pH	8.7		
Fatty acid	65.30%	64.60%	ISO 685 (determination of total alkali content and total fatty matter content)
Moisture	5.60%	5.00%	ISO 672 (determination of moisture and volatile matter content)
Combined alkali	8.85%	8.85%	ISO 456 (determination of free caustic alkali)
Chloride	3.70%	3.90%	ISO 457 (determination of chloride content—Titrimetric method)
Free alkali	0.10%	0%	ISO 684 (determination of total free alkali)
Glycerol	0.70%	0.70%	ISO 1066 (determination of glycerol content—Titrimetric method)

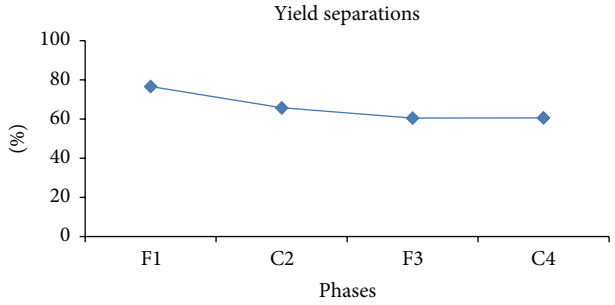

Figure 4: Yield of four crystallizations.

3.1. Separation Yield. To know the efficiency of our process, we have made a calculation of yield's various crystallization stages according to the following relation:

$$Y = \left(\frac{(\text{mass ester} * \text{purity})}{(\text{initial mass} * \text{initial purity})} \right) * 100. \quad (1)$$

As a result we have found 46.98 g esters with a purity of about 95.49%. We can say that the yield of our method is very satisfying since we could reach a value of 60.61%, and we also see after the calculation of yield of other separations the results are very important because we have had results that exceed 60% (Figure 4).

3.2. Saponification Yield. From 150 mL (138 g) of oil we could produce approximately 141.67 g soap whose characteristics are presented in Table 6.

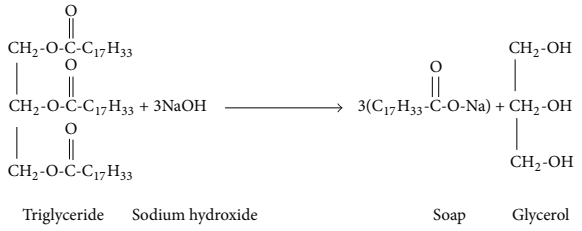

(2)

We accept as data

M (oil) = 884 g/mol and M (soap) = 304 g/mol

and n (oil) = n (soap)/3

m (oil)/M (oil) = m (soap)/3 $*$ M (soap)

Table 7: Characteristics of the resulting glycerol.

Parameters	Literature [63]	Values
Density	1.26	1.263
Boiling point (°C)	290	290
Melting point (°C)	17-18	17.5

with m (oil) = 138 g and m (soap) experimental = 141.67 g

m (soap) theoretical = 3 $*$ 304 $*$ 138/884 = 142.37 g

$$Y = \left(\frac{m\,(\text{soap})\,\text{exp}}{m\,(\text{soap})\,\text{th}} \right) * 100$$
$$Y = \left(\frac{141.67}{142.37} \right) * 100 = 99.50\%. \quad (3)$$

The yield of saponification was determined to know the efficiency of our process, seeking to improve it more by the optimization of operating conditions; 0.5% yield losses can have various causes: parasitic reactions, losses at the various stages of the synthesis (filtration, drying, and crystallization).

The saponification reaction allowed having a soap light beige color with a clean look smooth to the touch with abundant and consistent foam.

A comparison of the characteristics of soap obtained with those relating to soap made from olive pomace [63] showed that the values are quite comparable.

Glycerol derived from the saponification reaction and the transesterification is a viscous liquid, which is transparent, with a sweet taste whose characteristics are shown in Table 7.

Glycerin is soluble in water and in alcohols, very stable under normal conditions of use, and nontoxic and has no negative impact on the environment.

By comparing our glycerol and that produced by the method described in [63], we observe that both have the same characteristics, even if they do not belong to the same origin.

From 138 g of olive oil we could produce 9.14 g of glycerol by saponification, and from 184 g we were able to get 11.31 g by transesterification.

According to the results found in our process, an overall recovery diagram can be proposed (Figure 5).

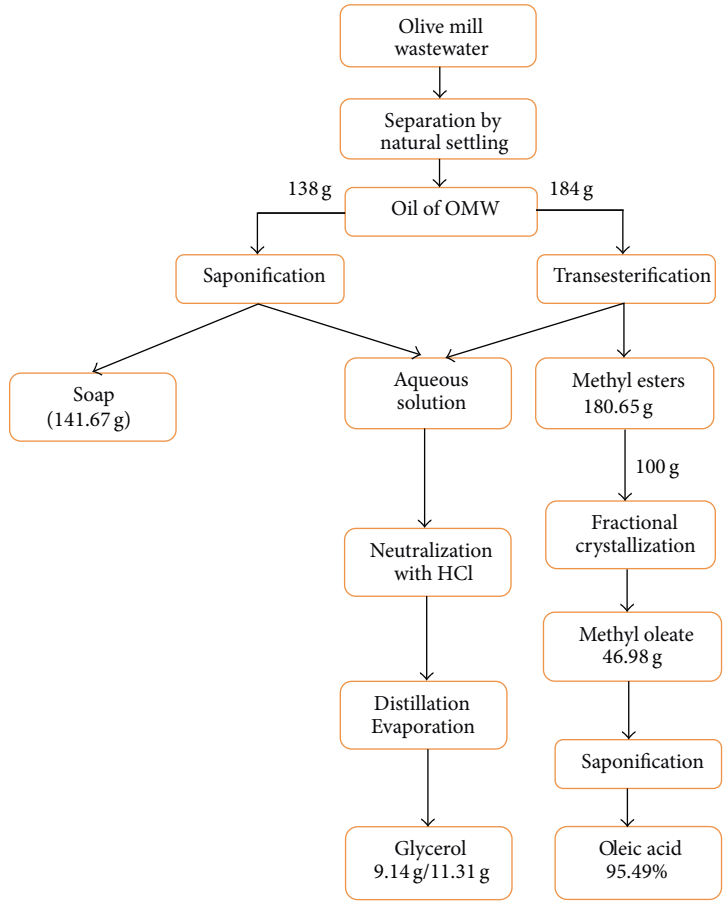

Figure 5: General diagram of the process.

4. Conclusions

In this work, it was possible to recover valuable products from a food waste that causes detrimental effects on nature.

In the first part, we have separated our oil from the olive mill wastewater collected, just by natural decantation. And we could extract oleic fatty acid as a product with a very important commercial value, by fractional crystallization in laboratory scale that we could separate it with a high purity of 95.49%.

The second part of this work was intended to saponify this poor nutritional quality oil to produce good quality soap and for the preparation of glycerin used in several areas.

In this work, we performed a quick and easy process for extracting a very expensive fatty acid market from olive oil wastewater with an easy method Instead of its preparation from olive oil.

Conflict of Interests

The authors declare that there is no conflict of interests regarding the publication of this paper.

References

[1] *Newsletter—Olive Market No. 91—February 2015*, International Olive Council, 2015.

[2] Ministry of Agriculture and Maritime Fishing of Morocco, Strategy Department and Statistics Strategic no. 95 Business intelligence-Olive sector in September 2013.

[3] I. El Mouhtadi, M. Agouzzal, and F. Guy, "L'olivier au Maroc," *Oilseeds and Fats, Crops and Lipids*, vol. 21, no. 2, article D203, 2014.

[4] A. K. M. M. B. Chowdhury, M. K. Michailides, C. S. Akratos, A. G. Tekerlekopoulou, S. Pavlou, and D. V. Vayenas, "Composting of three phase olive mill solid waste using different bulking agents," *International Biodeterioration & Biodegradation*, vol. 91, pp. 66–73, 2014.

[5] J. Jauhiainen, J. A. Conesa, R. Font, and I. Martín-Gullón, "Kinetics of the pyrolysis and combustion of olive oil solid waste," *Journal of Analytical and Applied Pyrolysis*, vol. 72, no. 1, pp. 9–15, 2004.

[6] A. R. Tekin and A. C. Dalgiç, "Biogas production from olive pomace," *Resources, Conservation and Recycling*, vol. 30, no. 4, pp. 301–313, 2000.

[7] A. Sebban, A. Bahloul, M. Saadoune et al., "Schema de valorisation des grignons d'olives produits par les maasras marocaines," *Déchets Sciences & Techniques*, no. 34, pp. 39–43, 2004.

[8] J. Estaún, J. Dosil, A. Al Alami, A. Gimeno, and A. De Vega, "Effects of including olive cake in the diet on performance and rumen function of beef cattle," *Animal Production Science*, vol. 54, no. 10, pp. 1817–1821, 2014.

[9] P. Paraskeva and E. Diamadopoulos, "Technologies for olive mill wastewater (OMW) treatment: a review," *Journal of Chemical Technology and Biotechnology*, vol. 81, no. 9, pp. 1475–1485, 2006.

[10] S. Dermeche, M. Nadour, C. Larroche, F. Moulti-Mati, and P. Michaud, "Olive mill wastes: biochemical characterizations and valorization strategies," *Process Biochemistry*, vol. 48, no. 10, pp. 1532–1552, 2013.

[11] A. Esmail, H. Abed, M. Firdaous et al., "Physico-chemical and microbiological study of oil mill wastewater (OMW) from three different regions of Morocco (Ouazzane, Fes Boulman and Béni Mellal)," *Journal of Materials and Environmental Science*, vol. 5, no. 1, pp. 121–126, 2014.

[12] R. Borja, J. Alba, A. Mancha, A. Martin, V. Alonso, and E. Sánchez, "Comparative effect of different aerobic pretreatments on the kinetics and macroenergetic parameters of anaerobic digestion of olive mill wastewater in continuous mode," *Bioprocess Engineering*, vol. 18, no. 2, pp. 127–134, 1998.

[13] C. Paredes, M. P. Bernal, J. Cegarra, and A. Roig, "Bio-degradation of olive mill wastewater sludge by its co-composting with agricultural wastes," *Bioresource Technology*, vol. 85, no. 1, pp. 1–8, 2002.

[14] D. Mantzavinos and N. Kalogerakis, "Treatment of olive mill effluents. Part I. Organic matter degradation by chemical and biological processes—an overview," *Environment International*, vol. 31, no. 2, pp. 289–295, 2005.

[15] J. Beltrán-Heredia, J. Torregrosa, J. García, J. R. Domínguez, and J. C. Tierno, "Degradation of olive mill wastewater by the combination of Fenton's reagent and ozonation processes with an aerobic biological treatment," *Water Science and Technology*, vol. 44, no. 5, pp. 103–108, 2001.

[16] C. Paredes, M. P. Bernal, J. Cegarra, and A. Roig, "Bio-degradation of olive mill wastewater sludge by its co-composting with agricultural wastes," *Bioresource Technology*, vol. 85, no. 1, pp. 1–8, 2002.

[17] I. Aviani, Y. Laor, S. Medina, A. Krassnovsky, and M. Raviv, "Co-composting of solid and liquid olive mill wastes: management aspects and the horticultural value of the resulting composts," *Bioresource Technology*, vol. 101, no. 17, pp. 6699–6706, 2010.

[18] B. Zenjari, H. El Hajjouji, G. Ait Baddi et al., "Eliminating toxic compounds by composting olive mill wastewater-straw mixtures," *Journal of Hazardous Materials*, vol. 138, no. 3, pp. 433–437, 2006.

[19] L. Cooperband, *The Art and Science of Composting: A Resource for Farmers and Compost Producers*, University of Wisconsin-Madison, 2002.

[20] A. Roig, M. L. Cayuela, and M. A. Sánchez-Monedero, "An overview on olive mill wastes and their valorisation methods," *Waste Management*, vol. 26, no. 9, pp. 960–969, 2006.

[21] A. G. Vlyssides, M. Loizides, and P. K. Karlis, "Integrated strategic approach for reusing olive oil extraction by-products," *Journal of Cleaner Production*, vol. 12, no. 6, pp. 603–611, 2004.

[22] M. Hamdi, "Future prospects and constraints of olive mill wastewaters use and treatment: a review," *Bioprocess Engineering*, vol. 8, no. 5-6, pp. 209–214, 1993.

[23] E. Martilotti, *Use of Olive by-Products in Animal Feeding in Italy*, Division de la Production et de la Santé Animale. FAO, Rome, Italy, 1983.

[24] R. Sansoucy, X. Alibes, Ph. Berge, F. Martilotti, A. Nefzaoui, and P. Zoïopoulos, *Los Subproductos del Olivar en la Alimentación Animal en la Cuenca del Mediterráneo*, vol. 43 of *Producción y Sanidad Animal*, FAO, Rome, Italy, 1985.

[25] T. H. Erguder, E. Guven, and G. N. Demirer, "Anaerobic digestion of olive mill wastes in batch reactors," *Process Biochemistry*, vol. 36, pp. 243–248, 2000.

[26] J. Gelegenis, D. Georgakakis, I. Angelidaki, N. Christopoulou, and M. Goumenaki, "Optimization of biogas production from olive-oil mill wastewater, by codigesting with diluted poultry-manure," *Applied Energy*, vol. 84, no. 6, pp. 646–663, 2007.

[27] G. N. Demirer, M. Duran, E. Güven, Ö. Ugurlu, U. Tezel, and T. H. Ergüder, "Anaerobic treatability and biogas production potential studies of different agro-industrial wastewaters in Turkey," *Biodegradation*, vol. 11, no. 6, pp. 401–405, 2000.

[28] A. Nefzaoui, "Valorisation des sous-produits de l'olivier," in *Fourrages et Sous-Produits Méditerranéens*, J.-L. Tisserand and X. Alibés, Eds., Options Méditerranéennes: Série A. Séminaires Méditerranéens no. 1, pp. 101–108, CIHEAM, Zaragoza, Spain, 1991.

[29] E. S. Aktas, S. Imre, and L. Ersoy, "Characterization and lime treatment of olive mill wastewater," *Water Research*, vol. 35, no. 9, pp. 2336–2340, 2001.

[30] M. Uğurlu and İ. Kula, "Decolourization and removal of some organic compounds from olive mill wastewater by advanced oxidation processes and lime treatment," *Environmental Science and Pollution Research*, vol. 14, no. 5, pp. 319–325, 2007.

[31] A. Ginos, T. Manios, and D. Mantzavinos, "Treatment of olive mill effluents by coagulation-flocculation-hydrogen peroxide oxidation and effect on phytotoxicity," *Journal of Hazardous Materials*, vol. 133, no. 1–3, pp. 135–142, 2006.

[32] N. Adhoum and L. Monser, "Decolourization and removal of phenolic compounds from olive mill wastewater by electrocoagulation," *Chemical Engineering and Processing: Process Intensification*, vol. 43, no. 10, pp. 1281–1287, 2004.

[33] A. S. Fajardo, R. F. Rodrigues, R. C. Martins, L. M. Castro, and R. M. Quinta-Ferreira, "Phenolic wastewaters treatment by electrocoagulation process using Zn anode," *Chemical Engineering Journal*, vol. 275, pp. 331–341, 2015.

[34] C. Belaid, M. Khadraoui, S. Mseddi, M. Kallel, B. Elleuch, and J. F. Fauvarque, "Electrochemical treatment of olive mill wastewater: treatment extent and effluent phenolic compounds monitoring using some uncommon analytical tools," *Journal of Environmental Sciences*, vol. 25, no. 1, pp. 220–230, 2013.

[35] Codex Alimentarius, "Codex standard for olive oils and olive pomace oils," CODEX STAN 33-1981.Rev. 2-2003, Commission of the Codex Alimentarius, 2009.

[36] ISO660, "International norm, Animal and Vegetable fats and oils: determination of acid value and acidity," 1996.

[37] ISO, "International norm, animal and vegetable fats and oils—determination of iodine value," ISO 3961, 2009.

[38] ISO 3960, International norm, Animal and Vegetable fats and oils, Determination of peroxide value, 2001.

[39] ISO, "International norm, animal and vegetable fats and oils—determination of saponification value," ISO 3657, 2013.

[40] ISO, *International Norm, Animal and Vegetable Fats and Oils. Determination of Refractive Index*, ISO 6320, 4th edition, 2000.

[41] ISO, "International norm, analysis of soaps—determination of total alkali content and total fatty matter content," ISO 685, 2010.

[42] ISO 672, International norm, Analysis of soaps, Determination of moisture and volatile matter content, 2010.

[43] ISO 456, International norm, Analysis of soaps, Determination of free caustic alkali, 2010.

[44] ISO, "International norm, analysis of soaps. Determination of chlorie content—titrimetric method," ISO 457, 2010.

[45] ISO 684, International norm, Analysis of soaps, Determination of total free alkali, 2010.

[46] ISO 1066, International norm, Analysis of soaps, Determination of glycerol content—Titrimetric method, 2010.

[47] N. Q. Wu, L. Fu, M. Su, M. Aslam, K. C. Wong, and V. P. Dravid, "Interaction of fatty acid monolayers with cobalt nanoparticles," *Nano Letters*, vol. 4, no. 2, pp. 383–386, 2004.

[48] T. Murakami, M. Yoshioka, R. Yumoto et al., "Topical delivery of keloid therapeutic drug, tranilast, by combined use of oleic acid and propylene glycol as a penetration enhancer: evaluation by skin microdialysis in rats," *Journal of Pharmacy and Pharmacology*, vol. 50, no. 1, pp. 49–54, 1998.

[49] A. Alegría and J. Cuellar, "Esterification of oleic acid for biodiesel production catalyzed by 4-dodecylbenzenesulfonic acid," *Applied Catalysis B: Environmental*, vol. 179, pp. 530–541, 2015.

[50] M. Loury, Les procédés physiques de séparation. Séparation par changement d'état: distillation, entrainement, cristallisation, inclusion. Journées Inform, Méth. Instrum. Anal. Contrôle Corps gras Prod. App., Paris, 27–31 mai, 59–70, 1968.

[51] K. E. Murray, "Low pressure fractional distillation and its use in the investigation of lipids," in *Progress in the Chemistry of Fats and Other Lipids*, vol. 3, pp. 244–273, Pergamon Press, London, UK, 1955.

[52] D. Swern and W. E. Parker, "Application of urea complexes in the purification of fatty acids, esters, and alcohols. II. Oleic acid and methyl oleate from olive oil," *Journal of the American Oil Chemists Society*, vol. 29, no. 12, pp. 614–615, 1952.

[53] J. G. Keppler, S. Sparreboom, J. B. Stroink, and J. D. Von Mikusch, "A note on the preparation of pure oleic and linoleic acid," *Journal of the American Oil Chemists' Society*, vol. 36, no. 7, pp. 308–309, 1959.

[54] L. Frémont and M.-T. Gozzelino, "Préparation d'acide oléique a 99,5 p. 100 de pureté," *Annales de Biologie Animale, Biochimie, Biophysique*, vol. 13, no. 4, pp. 691–697, 1973.

[55] S. Kitane, A. Sebban, A. Bahloul, and J. L. Pineau, "Procédé écologique de traitement et de valorisation de rejets solides et des margines," Tech. Rep. 29150 à l'OMPIC, 2006.

[56] A. Rywińska, W. Rymowicz, B. Zarowska, and M. Wojtatowicz, "Biosynthesis of citric acid from glycerol by acetate mutants of Yarrowia lipolytica in fed-batch fermentation," *Food Technology and Biotechnology*, vol. 47, no. 1, pp. 1–6, 2009.

[57] N. Gontard, S. Guilbert, and J.-L. Cuq, "Water and glycerol as plasticizers affect mechanical and water vapor barrier properties of an edible wheat gluten film," *Journal of Food Science*, vol. 58, no. 1, pp. 206–211, 1993.

[58] M. Hara and A. S. Verkman, "Glycerol replacement corrects defective skin hydration, elasticity, and barrier function in aquaporin-3-deficient mice," *Proceedings of the National Academy of Sciences of the United States of America*, vol. 100, no. 12, pp. 7360–7365, 2003.

[59] J. Mattai, C. L. Froebe, L. D. Rhein et al., "Prevention of model stratum corneum lipid phase transitions *in vitro* by cosmetic additives—differential scanning calorimetry, optical microscopy, and water evaporation studies," *Journal of the Society of Cosmetic Chemists*, vol. 44, no. 2, pp. 89–100, 1993.

[60] S. Kitane, A. Sebban, and A. Bahloul, "Procédé et schéma de traitement pour la valorisation de déchets agro-alimentaires: fabrication de savon biodegradable du furfural de la glycérine et de charbon actif à partir des grignons d'olive," Tech. Rep. 27014, OMPIC, 2003.

[61] A. Godard, P. De Caro, S. Thiebaud-Roux, E. Vedrenne, and Z. Mouloungui, "New environmentally friendly oxidative scission of oleic acid into azelaic acid and pelargonic acid," *Journal of the American Oil Chemists' Society*, vol. 90, no. 1, pp. 133–140, 2013.

[62] S. E. Turnwald, M. A. Lorier, L. J. Wright, and M. R. Mucalo, "Oleic acid oxidation using hydrogen peroxide in conjunction with transition metal catalysis," *Journal of Materials Science Letters*, vol. 17, no. 15, pp. 1305–1307, 1998.

[63] A. Nefzaoui, "Contribution à la rentabilité de l'oléiculture par la valorisation optimale des sous-produits, séminaire sur l'économie de l'olivier. Tunis," Science et Technique, Olivae n°19, Janvier 1987.

Hindawi Publishing Corporation
BioMed Research International
Volume 2015, Article ID 832571, 6 pages
http://dx.doi.org/10.1155/2015/832571

Research Article

Cadmium Removal from Aqueous Systems Using *Opuntia albicarpa* L. Scheinvar as Biosorbent

Rosa Icela Beltrán-Hernández,[1] Gabriela Alejandra Vázquez-Rodríguez,[1] Luis Felipe Juárez-Santillán,[1] Ivan Martínez-Ugalde,[2] Claudia Coronel-Olivares,[1] and Carlos Alexander Lucho-Constantino[1]

[1]*Centro de Investigaciones Químicas, Universidad Autónoma del Estado de Hidalgo, Carretera Pachuca-Tulancingo Km 4.5, Ciudad Universitaria, 42067 Pachuca, HGO, Mexico*
[2]*Programa de Ingeniería en Biotecnología, Universidad Politécnica de Pachuca, Ex-Hacienda de Santa Bárbara, Carretera Pachuca-Ciudad Sahagún Km 20, 43830 Zempoala, HGO, Mexico*

Correspondence should be addressed to Carlos Alexander Lucho-Constantino; a_lucho@yahoo.com.mx

Received 17 September 2015; Revised 21 November 2015; Accepted 22 November 2015

Academic Editor: Basel Khraiwesh

The aim of this research was to investigate the use of a natural adsorbent like nopal (*Opuntia albicarpa* L. Scheinvar) for removing cadmium from aqueous solutions with low concentrations of this metal. Two treatments were applied to the cladodes: a dehydration to get dehydrated nopal (DHN) and heating up to 90°C to obtain a thermally treated nopal (TN). After examining the effect of various pH values (2–7), the capacity of each biosorbent was examined in batch sorption tests at different dosages (0, 500, 1000, 1500, 2000, and 3000 mg L^{-1}). The results indicated that adsorption of cadmium to biomass of DHN and TN was highly dependent on pH and biosorbent dosage. The best removal of cadmium (53.3%, corresponding to q_e of 0.155 mg g^{-1}) was obtained at pH 4.0 by using the TN sorbent. Infrared and Raman spectra confirmed that cadmium removal occurred via adsorption to –OH functional groups.

1. Introduction

Heavy metals receive world attention due to their long-term effects in the environment. Some of them, such as cadmium, are only found at trace level in the terrestrial crust. However, heavy metals are widely used in industrial processes and in commonly used goods, thereby increasing their presence and concentration in aquatic systems [1].

Cadmium has been classified into Group B1 as a probable human carcinogen by the US Environmental Protection Agency (EPA) and as a group I carcinogen by the International Agency for Research in Cancer (IARC) [2]. Consequently, World Health Organization, EPA, and the European Drinking Water Directive have established 0.005 mg L^{-1} as the maximum standard for Cd in water for municipal supply. In wastewater, EPA has set an upper limit of 2 mg L^{-1} in the Cd concentration before discharge to receiving water bodies [3].

Conventionally, heavy metals have been removed from wastewater by processes including chemical precipitation, coagulation/flocculation, flotation, ion exchange resins, absorption, and membrane filtration. However, the running costs of these processes are disadvantageous, as well as the generation of chemical sludges in the case of chemical precipitation [1, 4, 5].

Biosorption constitutes a low-cost and feasible method to remove heavy metals from aqueous streams. By using cheap and naturally abundant materials, this technology is well-suited for local and full-scale applications. Biosorbents such as living or dead microbial biomass, seaweeds, agricultural wastes, sawdust, and modified cellulosic materials have been studied for metal removal [1, 4–6].

In developing countries, the abundance and inexpensive nature of agricultural wastes make them a promising alternative to conventional chemical processes for heavy metal removal. Moreover, these natural sorbents yield biodegradable sludges and offer the possibility of metal recovering. Among the natural materials investigated with this purpose, nopal cladodes (*Opuntia* sp.) have been reported to have a high potential for removal of turbidity [7], ions from mine drainage [8], lead [9], and chromium [10]. Several biosorbents have been used for removing cadmium, and they have been shown to be a feasible alternative because high efficiencies and adsorption capacities (q_e) have been obtained when elevated concentrations of cadmium (even as high as 1 g L^{-1}) were tested [1].

This paper reports the removal of low concentrations of cadmium from aqueous media by using cladodes of *Opuntia albicarpa* L. Scheinvar. The objective of testing low concentrations was to simulate more common conditions, that is, cadmium levels comparable to the upper limit of 2 mg L^{-1} established for wastewater by EPA [3]. Two biosorbent preparation methods were tested in terms of removal efficiency. Additionally, functional groups interacting with cadmium were identified by using FTIR and Raman spectroscopy.

2. Materials and Methods

2.1. Cadmium Solutions. A stock cadmium solution (10000 mg Cd^{2+} L^{-1}) was prepared by dissolving 1 g of metallic cadmium (99.9% of purity, Sigma Aldrich) in 20 mL of concentrated HNO_3. The solution volume was completed up to 100 mL with deionized water (Milli Q Plus Millipore Columns Systems). Cadmium solutions (1.6 ± 0.02 mg Cd^{2+} L^{-1}) used in biosorption studies were made by appropriate dilution of the stock solution with deionized water.

2.2. Natural Materials. Nopal specimens of *Opuntia albicarpa* L. Scheinvar were collected from Zempoala (Hidalgo, Mexico), and only one-year aged cladodes were retained for the study. Prior to treatment, cladodes were washed with deionized water and cut in 3 cm × 1 cm segments of about 10 g each.

2.3. Biosorbent Preparation. Biosorbents were obtained following two different treatments. Dehydrated nopal (DHN) was prepared by drying cladode segments at 70°C for 5 h. In this way, a reduction of 82.7% of the total water content could be achieved. Next, cladodes were ground using an electric blender (Waring, USA) and sieved through 250–600 μm mesh screens (Tyler test sieves #60 and #30, resp.).

Thermally treated nopal (TN) was prepared by heating segments of cladodes (200 g in total) with 500 mL of water until boiling occurred (approximately to 90°C at about 2000 meters above sea level). Then, the bulk mixture was liquefied and dehydrated at 70°C for 24 h. Dried nopal was ground and sieved to obtain a particle size lower than 600 μm.

2.4. Biosorption Tests. Batch sorption tests were carried out in triplicate on a standard jar test apparatus (Quimipura, Mexico). Each jar was filled with 500 mL of cadmium solution (of about 2 mg Cd^{+2} L^{-1}) and then stirred at 150 rpm for 1 min. Stirring speed was then lowered to 85 rpm for 4 min and after set to 20 rpm during 10 min. Finally, samples were allowed to settle for 30 min [11]. The sorbent was recovered by filtration of the settled material through Whatman 42 filter paper.

To assess cadmium removal, supernatant samples (taken before and after a given treatment) were digested in a microwave oven (MARSX-5) by following a standard technique [12]. Subsequently, samples were analyzed in an Atomic Absorption Spectrophotometer (AAS, Varian 800).

The effect of pH on cadmium removal was studied at different pH values (2–7) of the cadmium solution and with 500 mg L^{-1} of DHN. pH was adjusted by adding 1.0 M HCl or 1.0 M NaOH. The effect of the biosorbent dosage was studied at five doses (500, 1000, 1500, 2000, and 3000 mg L^{-1}) of both biosorbents.

2.5. Modeling of Biosorption. Percentages of cadmium removal were adjusted to the Chapman sigmoidal expression:

$$\%\ \text{Cd removal} = a\left(1 - e^{-b \cdot m}\right)^{c}, \quad (1)$$

where a is the maximum percentage of Cd removal, m is the dosage of biosorbent, and b and c are empirical constants. Curve fitting was carried out using SigmaPlot for Windows version 12.0 (Systat Software, Inc.).

2.6. FTIR and Raman Spectroscopy Analyses. Before and after being used in the jar tests, biosorbents were screened by Fourier transform infrared (FTIR) spectroscopy (Perkin Elmer Spectrum GX) using the KBr pellet method.

Raman spectra were obtained on a Perkin Elmer Spectrum GX, equipped with a Raman module attachment, a Nd^{3+} laser operating at 1064 nm in the near infrared, and a InGaAs detector cooled with liquid N_2. The spectral resolution used was 4 cm^{-1}. Samples of biosorbents were prepared in the same way (KBr pellet) as for FTIR analyses. Likewise, biosorbents were analyzed before and after being used in jar tests.

3. Results and Discussion

3.1. Effect of pH on Biosorption. Since pH of aqueous media is an important parameter controlling adsorption processes of heavy metals [16], the effectiveness of DHN biosorbent was examined at different initial pH values (2–7). The initial cadmium contents comprised between 1.593 and 1.806 mg L^{-1}. After the jar tests, concentrations of cadmium comprising between 1.32 and 1.63 mg L^{-1} were measured. Figure 1 shows the results in terms of cadmium removal percentages and adsorption capacity (q_e, mg Cd adsorbed g^{-1} biosorbent). On the one hand, the lower cadmium removal observed at pH 2 suggests a competition between Cd^{2+} and H^+ for the adsorption sites. On the other hand, the greatest cadmium removal (18.5%, corresponding to q_e of 0.327 mg g^{-1}) was registered at pH 4. Barrera et al. [8] reported that the uptake of Cr(III) and Cr(VI) in acid mine drainage by *Opuntia* sp. was maximum at pH 4 (99 and 77%, resp.). Similarly, a pH

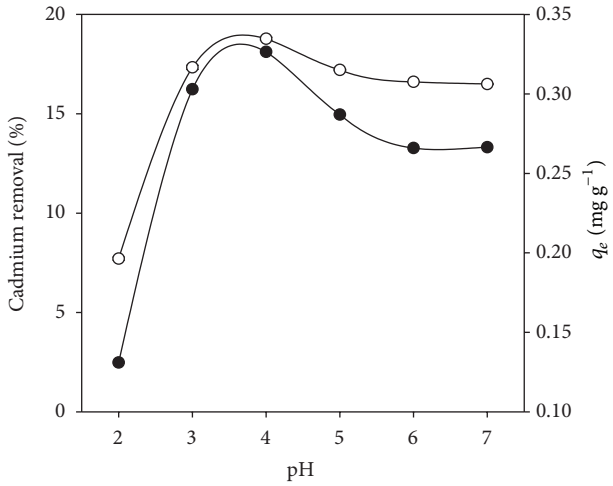

Figure 1: Effect of pH on cadmium removal by dehydrated nopal (DHN). (-○-) Percentage of cadmium removal; (-●-) q_e, adsorption capacity [mg Cd adsorbed g^{-1} biosorbent].

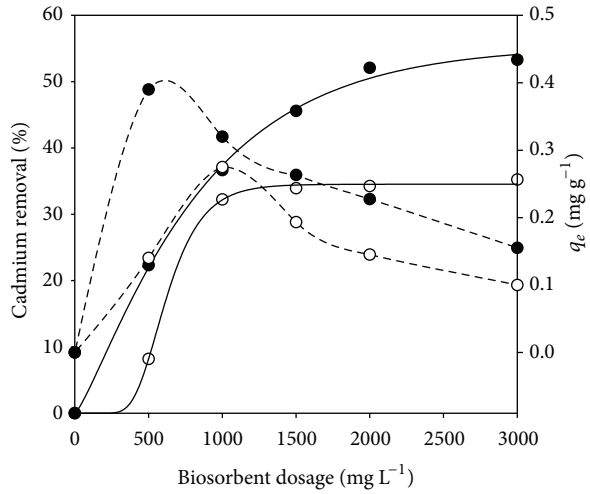

Figure 2: Effect of biosorbent dosage on cadmium removal. (-○-) DHN; (-●-) TN. The continuous lines represent the modeling of the percentages of cadmium removal. The dashed lines represent the progression of q_e, adsorption capacity [mg Cd adsorbed g^{-1} biosorbent].

range of 3–5 allowed a higher amount of Pb^{2+} to be adsorbed by *Opuntia streptacantha* [9]. Fernández-López et al. [10] also found that the adsorption of hexavalent chromium by *Opuntia* cladodes is pH dependent and maximum at pH 2. Consequently, an acidic pH value of 4 was used in further testing of the biosorbents.

3.2. Effect of Biosorbent Dosage on Cadmium Removal. The effect of varying the dosage of both biosorbents (DHN and TN) from 500 to 3000 mg L^{-1} at pH 4 is shown in Figure 2. For DHN tests, the initial cadmium concentration was 1.69 mg L^{-1}. At the end of jar tests, cadmium contents comprised between 1.09 and 1.55 mg L^{-1}. The cadmium uptake increased from 8.1 to 35.2% when the dose of sorbent was raised from 500 to 1000 mg L^{-1}. The measured value of q_e also varied (from 0.14 to 0.275 mg g^{-1}) along with the increase of the biosorbent dose. Further increases of the dose of biosorbent led to a diminution of q_e (equivalent to 0.1 mg g^{-1} for a dosage of 3000 mg L^{-1}). Barka et al. [15] tested dehydrated *Opuntia ficus* for removing high contents of cadmium (30–300 mg L^{-1}), and they obtained efficiencies comprised between 10.49 and 36.71% by using 500–4000 mg L^{-1} of biosorbent, respectively. Apparently, the use of dehydrated *Opuntia* sp. at these doses leads to low-to-moderate removal efficiencies to be obtained. In fact, biosorbents used for removing low cadmium concentrations (1–10 mg L^{-1}) generally bring about low-to-moderate removal efficiencies [1, 13–15], which is in agreement with our results (Table 1).

For TN tests, the initial cadmium concentration was 1.74 mg L^{-1}. After the jar tests, cadmium contents were comprised between 0.81 and 1.35 mg L^{-1}. The increase of biosorbent dosage from 500 to 2000 mg L^{-1} increased cadmium uptake from 22.3 to 53.3% and diminished q_e from 0.39 to 0.155 mg g^{-1} (Figure 2). Presumably, enhancement of cadmium removal at higher biosorbent doses is due to an increase in adsorption sites. However, further increasing of biosorbent does not appear to be significant for improving cadmium removal.

The results obtained by simulation of the Chapman equation are also shown in Figure 2. The model appears to depict the experimental data adequately, because the Pearson correlation coefficients (r^2) were 0.998 and 0.999 for TN and DHN, respectively. The a value of (1), corresponding to the maximum percentage of Cd removal, was 55.4 and 34.5, respectively, and so the adsorption capacity of the biosorbent was enhanced by the thermal treatment. The b and c values were 0.0013 and 1.287 for TN results, respectively. For DHN, b and c were found to be 0.006 and 27.92, respectively.

3.3. FTIR Spectra of Biosorbents. The main functional groups involved in biosorption are binding groups located on the surface of cell wall, as carboxyl, sulfonate, phosphate, amino, amide, and imidazole [16]. Infrared spectroscopy allows the identification of these moieties, as well as the detection of changes in their vibrational modes due to bond formation.

Figure 3 shows FTIR spectra of DHN before and after contact with a Cd solution at pH 4. Before exposition to cadmium, the spectrum of DHN sorbent showed tension bands at 3432 and 2924 cm^{-1}, corresponding to O–C and C–H bonds, respectively. C=O tension bands were observed too, but at a lower frequency (1650 cm^{-1} instead 1700 cm^{-1}). This can arise from mutarotation changes of ketomoieties into aldehyde or alcohol groups in biosorbent sugars, which are likely to diminish the tension in the C=O bond. The band found at 1623 cm^{-1} is assigned to C=O stretching in amide groups. Finally, in the range of 1318–1036 cm^{-1}, the bands pointed to C–N and C–O stretching or deformation vibrations of –CH, –OH, or –NH bonds. Table 2 summarizes the association between infrared adsorption frequencies and functional groups observed in FTIR spectra of biosorbents (DHN and TN), which could be responsible for cadmium removal.

Table 1: Cadmium removal by biosorption.

Bioadsorbent	$[Cd]_i$ (mg L^{-1})	Sorption capacity[a] (mg/g) or removal efficiency[b] (%)	Experimental conditions	Reference
Rice husk	11.24	26.73[a]	[B] = 500 mg L^{-1} T = 25°C pH = 2.0–6.0	[13]
Olive tree pruning waste	1–10	36.6[a]	[B] = 100 mg L^{-1} pH = 5.5 T = 21 ± 0.4°C t = 120 min	[14]
Dried cladodes (*Opuntia ficus*)	30–300	12.07–30.42[a] 10.5–36.7[b]	[B] = 500–4000 mg L^{-1} pH = 2.3–6.5 T = 25–60°C	[15]
Dehydrated nopal (DHN) of *Opuntia albicarpa* L. Scheinvar	1.6	0.14–0.275[a] 8.1–35.2[b]	[B] = 500–1000 mg L^{-1} pH 4.0	This study
Thermally treated nopal (TN) *Opuntia albicarpa* L. Scheinvar	1.6	0.39–0.23[a] 22.3–53.3[b]	[B] = 500–2000 mg L^{-1} pH 4.0	This study

$[Cd]_i$: initial cadmium concentration, [B]: dosage of biosorbent.

Table 2: Functional groups present in treated *Opuntia albicarpa* L. Scheinvar and their corresponding infrared absorption frequencies.

Frequency (cm^{-1})	Assignment
3600	N–H amines groups
3428	Hydroxyl group
2850	C–H stretching
1623	C=O stretching of COOH
1414	Symmetric bending of CH_3
1317	C–N groups
1050	C–O groups

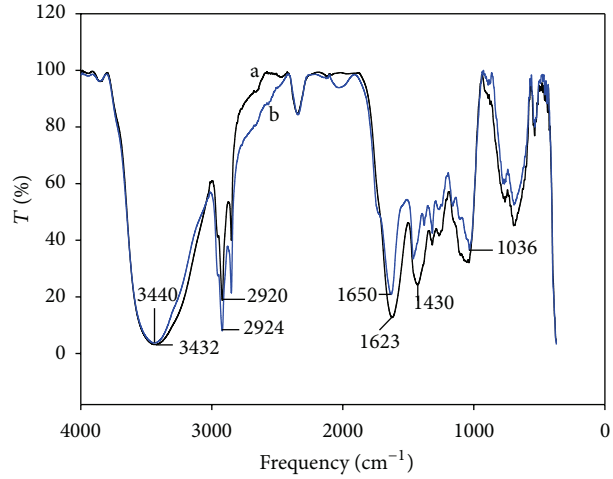

Figure 3: FTIR spectra of the dehydrated biosorbent (a) before and (b) after the jar tests.

After being in contact with the Cd solution, a light modification in the 3432–3440 cm^{-1} region (assigned to –OH and –NH bond stretching) was noticed. The bands in the 1623–1036 cm^{-1} range also showed a small displacement. These changes in the spectra could indicate Cd sorption to the DHN. Likewise, Gupta and Rastogi [17] showed Cd adsorption when *Oedogonium* sp. was used as biosorbent through shifts of the IR bands at 1082, 1650, and 2924 cm^{-1}.

Thermally treated nopal showed a strong interaction with cadmium (Figure 4). After adsorption tests, bands at 2900–3600 cm^{-1} region (assigned to –OH and –NH groups) exhibited a lower intensity, possibly due to presence of Cd in these sites. Band intensity in the 1634–1034 cm^{-1} region also diminished after the exposure to Cd. In Figure 5, functional groups of the thermally treated nopal are compared against those of the dehydrated biosorbent. In a general manner, the TN sorbent produced bands of lower intensities than those of dehydrated nopal, even though the later allowed a higher cadmium removal.

3.4. Raman Spectra of Biosorbents. As FTIR spectra did not indicate the presence of formal bonds, Raman spectroscopy was used to characterize superficial interactions between biosorbents and Cd.

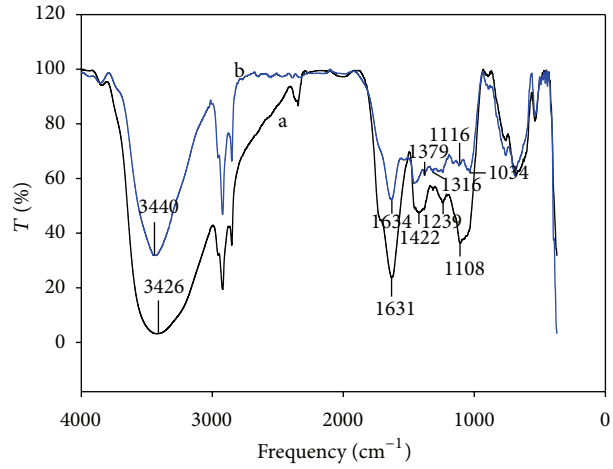

Figure 4: FTIR spectra of the thermally treated nopal (a) before and (b) after the jar tests.

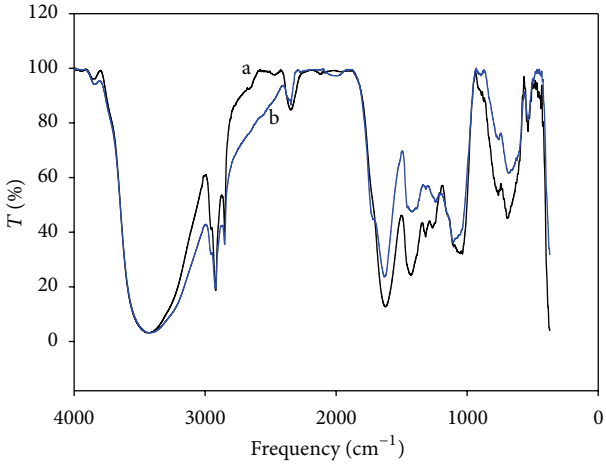

Figure 5: Comparison of FTIR spectra of the dehydrated biosorbent (a) before and (b) after the jar tests.

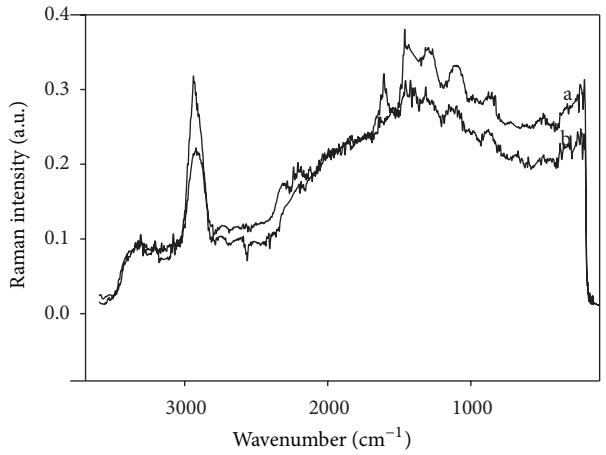

Figure 6: Raman spectra of the dehydrated biosorbent (a) before and (b) after the jar tests.

Figure 6 shows the spectrum of DHN biosorbent before and after being in contact with Cd. Bands assigned to C=O (1690 cm^{-1}), COO–H (1690 and 1615 cm^{-1}, with scissor vibration), and C–C (1558–1535 cm^{-1}) groups were detected, as well as an intense C–H band at 3045–3035 cm^{-1}. The band at 3000 cm^{-1} is probably due to –OH moieties and water [18]. Also, less-intense bands at 1088–1062 cm^{-1} (in-plane) and at 1033–1027 cm^{-1} (out-of-plane, deformation) were observed. Such bands, although less intense, were also present after adsorption tests, indicating a weak adsorption of Cd on DHN sorbent. The rest of the bands were superimposed and less defined than that of the C–H bond, which is understandably the main functional group in compounds present in *Opuntia albicarpa* L. Scheinvar.

Treated TN showed the same bands as DHN when sorbents were analyzed by Raman spectroscopy prior to adsorption tests (Figure 7). However, after being exposed to Cd solution, these bands disappeared in TN. The lack of bond vibration indicated that cadmium was retained only on the biosorbent surface.

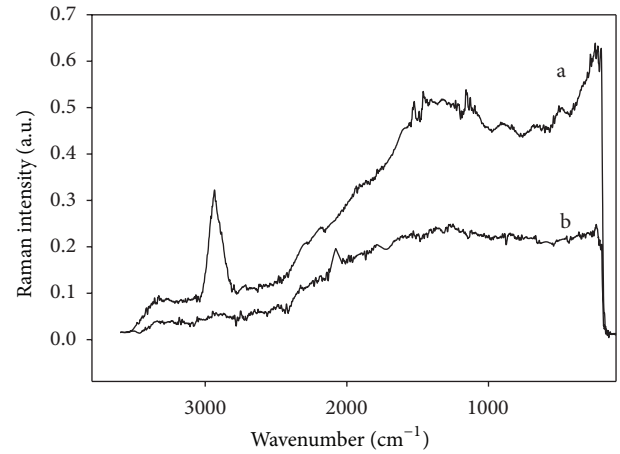

Figure 7: Raman spectra of the thermally treated biosorbent (a) before and (b) after the jar tests.

4. Conclusions

Thermally treated *Opuntia albicarpa* L. Scheinvar biomass presented the best removal of cadmium in biosorption studies. Metal adsorption was highly dependent on the pH and biosorbent dosage. IR and Raman spectra confirmed that the removal of cadmium occurred via adsorption and showed the interaction between cadmium and some functional groups (O–H, N–H, N–C=O, C–O, and C–N). Since nopal is a natural material widely distributed around the world, and the preparation of the TN biosorbent is easy and inexpensive, it could constitute an adequate metal removal technology for developing countries.

Conflict of Interests

The authors declare that there is no conflict of interests.

Acknowledgment

The authors owe special thanks to Professor Alejandro Álvarez Hernández (Universidad Autónoma del Estado de Hidalgo) for his kind help to analyze the IR spectra presented here and to improve the English of the paper.

References

[1] D. Purkayastha, U. Mishra, and S. Biswas, "A comprehensive review on Cd(II) removal from aqueous solution," *Journal of Water Process Engineering*, vol. 2, pp. 105–128, 2014.

[2] J. C. Nva Merrill, J. J. P. Morton, and S. D. Soileau, "Metals: cadmium," in *Principles and Methods of Toxicology*, A. W. Hayes, Ed., pp. 665–667, Taylor & Francis, London, UK, 2001.

[3] EPA, "Council directive of 16 June 1975 concerning the quality required of surface water intended for the abstraction of drinking water in the Member States," EPA 75/440/EEC, 2013.

[4] S. Karthikeyan, R. Balasubramanian, and C. S. P. Iyer, "Evaluation of the marine algae *Ulva fasciata* and *Sargassum* sp. for the biosorption of Cu(II) from aqueous solutions," *Bioresource Technology*, vol. 98, no. 2, pp. 452–455, 2007.

[5] A. Li, J. Zhang, and A. Wang, "Utilization of starch and clay for the preparation of superabsorbent composite," *Bioresource Technology*, vol. 98, no. 2, pp. 327–332, 2007.

[6] Y. Ding, D. Jing, H. Gong, L. Zhou, and X. Yang, "Biosorption of aquatic cadmium(II) by unmodified rice straw," *Bioresource Technology*, vol. 114, pp. 20–25, 2012.

[7] N. Fedala, H. Lounici, N. Drouiche, N. Mameri, and M. Drouiche, "Physical parameters affecting coagulation of turbid water with *Opuntia ficus-indica* cactus," *Ecological Engineering*, vol. 77, pp. 33–36, 2015.

[8] H. Barrera, F. Ureña-Núñez, B. Bilyeu, and C. Barrera-Díaz, "Removal of chromium and toxic ions presents in mine drainage by *Ectodermis* of *Opuntia*," *Journal of Hazardous Materials*, vol. 136, no. 3, pp. 846–853, 2006.

[9] P. Miretzky, C. Muñoz, and A. Carrillo-Chávez, "Experimental binding of lead to a low cost on biosorbent: Nopal (*Opuntia streptacantha*)," *Bioresource Technology*, vol. 99, no. 5, pp. 1211–1217, 2008.

[10] J. A. Fernández-López, J. M. Angosto, and M. D. Avilés, "Biosorption of hexavalent chromium from aqueous medium with opuntia biomass," *The Scientific World Journal*, vol. 2014, Article ID 670249, 8 pages, 2014.

[11] CSUSF, *Water Treatment Plant Operation—A Field Study Training Program*, California State University Sacramento Foundation, 3rd edition, 1996.

[12] EPA, "SW-846 EPA Test methods for evaluating solid waste physical/chemical method. Chapter Three—Metallic analytes. Method 3015 microwave assisted acid digestion of aqueous samples and extracts," CD-ROM Revision 3, US Environmental Protection Agency, Washington, DC, USA, 1995.

[13] G. Tan, H. Yuan, Y. Liu, and D. Xiao, "Removal of cadmium from aqueous solution using wheat stem, corncob, and rice husk," *Separation Science and Technology*, vol. 46, no. 13, pp. 2049–2055, 2011.

[14] O. Uzunosmanoglu, A. Uyanik, and M. S. Engin, "The removal of cadmium (II), copper (II) and lead (II) from aqueous solutions by olive tree pruning waste," *Fresenius Environmental Bulletin*, vol. 20, no. 12, pp. 3135–3140, 2011.

[15] N. Barka, M. Abdennouri, M. El Makhfouk, and S. Qourzal, "Biosorption characteristics of cadmium and lead onto eco-friendly dried cactus (*Opuntia ficus indica*) cladodes," *Journal of Environmental Chemical Engineering*, vol. 1, no. 3, pp. 144–149, 2013.

[16] K. Chojnacka, "Biosorption and bioaccumulation—the prospects for practical applications," *Environment International*, vol. 36, no. 3, pp. 299–307, 2010.

[17] V. K. Gupta and A. Rastogi, "Equilibrium and kinetic modelling of cadmium(II) biosorption by nonliving algal biomass *Oedogonium* sp. from aqueous phase," *Journal of Hazardous Materials*, vol. 153, no. 1-2, pp. 759–766, 2008.

[18] M. Oustromov, E. Fritsh, and S. Lefrant, "First data about the Raman spectroscopy of opals," *Revista Mexicana de Ciencias Geológicas*, vol. 1, pp. 73–83, 1999 (Spanish).